TUSKEGEE INSTITUTE

SCHOOL OF MECHANICAL ENGINEERING

TUSKEGEE INSTITUTE, ALABAMA

THIRD ANNUAL REPORT: HEAT PIPE RADIATORS FOR SPACE

CONTRACT NO. NAS9-13844(4S)

BY

JOHN P. SELLERS

SPONSORED BY

ENVIRONMENTAL AND THERMAL SYSTEMS SECTION

MANNED SPACECRAFT CENTER

NATIONAL AERONAUTICS AND SPACE ADMINISTRATION

HOUSTON, TEXAS

JANUARY, 1976

THIRD ANNUAL REPORT: HEAT PIPE RADIATORS FOR SPACE

BY

J. P. Sellers

Tuskegee Institute

Contract NAS9-13844 (Mod. 4S)

January 1976

FORWARD

This report was prepared for Johnson Space Center of the National Aeronautics and Space Administration. The work was performed under Contract NAS9-13844 with Mr. W. Ellis and Mr. B. French providing NASA guidance.

The work was performed from January 1975 to August 1975. The author would like to acknowledge the assistance of Mr. Nasir Awan, and to express his appreciation to Tuskegee Institute for granting permission to undertake the task.

ABSTRACT

Analysis of the data obtained by the Johnson Space Center on heat pipe radiator systems tested in both vacuum and ambient environments was continued. The systems included (a) a feasibility VCHP header heat-pipe panel, (b) the same panel reworked to eliminate the VCHP feature and referred to as the feasibility fluid header panel, and (c) an optimized flight-weight fluid header panel termed "the prototype".

The study included a description of freeze-thaw thermal vacuum tests conducted on the feasibility VCHP. In addition, the results of ambient tests made on the feasibility fluid header are presented including a comparison with analysis.

A thermal model of a fluid header heat pipe radiator was constructed and a computer program written. The program was used to make a comparison of the VCHP and fluid-header concepts for both single and multiple panel applications.

The computer program was also employed for a parametric study, including optimum feeder heat pipe spacing, of the prototype fluid header.

TABLE OF CONTENTS

LIST OF FIGURES

LIST OF TABLES

1.0 INTRODUCTION

This is the third annual report describing analytical effort under Contract NAS9-13844 in support of a NASA research investigation pertaining to heat pipe radiators for waste heat rejection in space. Earlier reports (1, 2) featured analytical and experimental comparisons of vacuum chamber data obtained on a feasibility VCHP header, 8ft x 4ft radiator panel, built and designed by Grumman Aerospace Corporation (3). Described in those reports were computer models for predicting steady state and transient performance of the radiator panel. NASA'S testing program included freezing and thawing of the panel; the description of that portion was not included in the first reports and is contained herein.

A major finding of the experimental program was that under most conditions the active portion of the VCHP header condenser was less than predicted which resulted in low heat transport compared to analysis. A plan designed to attack the problem on two fronts was initiated by NASA, hopefully to increase the low heat transport and/or determine its causes. Grumman designed and tested wick modifications while NASA was undertaking an ambient experimental investigation of the original feasibility VCHP. The NASA ambient test results are also discussed in the present report.

Neither of the two efforts were totally successful in establishing the precise cause of the VCHP low performance, hence NASA

directed Grumman to investigate alternate heat-pipe radiator designs. A concept proposed and accepted was the fluid header which was attractive because of its simplicity and low resistance to heat transfer. Control of the system it was proposed, could be provided by a by-pass in the Freon coolant line.

After NASA had directed Grumman to build a fluid header heat pipe radiator, a steady-state computer program model of it was written at Tuskegee for use in subsequent investigations. NASA also modified the feasibility VCHP header, converting it into a fluid header, and in a series of ambient tests an early evaluation of the concept was obtained. A brief discussion of those results is also contained herein.

2.0 FREEZE-THAW STUDY OF FEASIBILITY VCHP

The freeze-thaw experiment conducted in August 1973 consumed over 13 hours of the thermal vacuum total test period and occurred during the time period 193-16-12 to 194-06-15. The history of the controlled parameters T_{IN}, Q'_A and $\dot{m}$ during the experiment are presented in Figs. 2.1, 2.2, and 2.3.

With an environment of $Q'_A \approx 5.0$ Btu/hr-ft^2 and zero Freon flow, the panel was frozen after about three hours (193-19-00). Panel temperatures were less than -110°F.

An attempt was made to thaw the panel by turning on the flow and increasing the temperature of the Freon coolant. The VCHP header condenser temperature, Fig. 2.4, indicated that the header indeed thawed beginning at 193-22-30, but was refrozen shortly thereafter by the operator shutting off the Freon flow and lowering the Freon temperature. The feeder heat pipes had remained frozen.

At 194-02-25 thawing conditions were repeated, and as before the header functioned but at a minimal heat load level since the feeders again remained frozen. From these two thawing data points the Freon conditions for reactiveating the VCHP header from a frozen state ($T \approx -110°F$ and $Q'_A \approx 0$ Btu/hr-ft^2) were:

$$T_{IN} = 40 - 50°F$$

$$\dot{m} = 300 - 400 \text{ lb/hr}$$

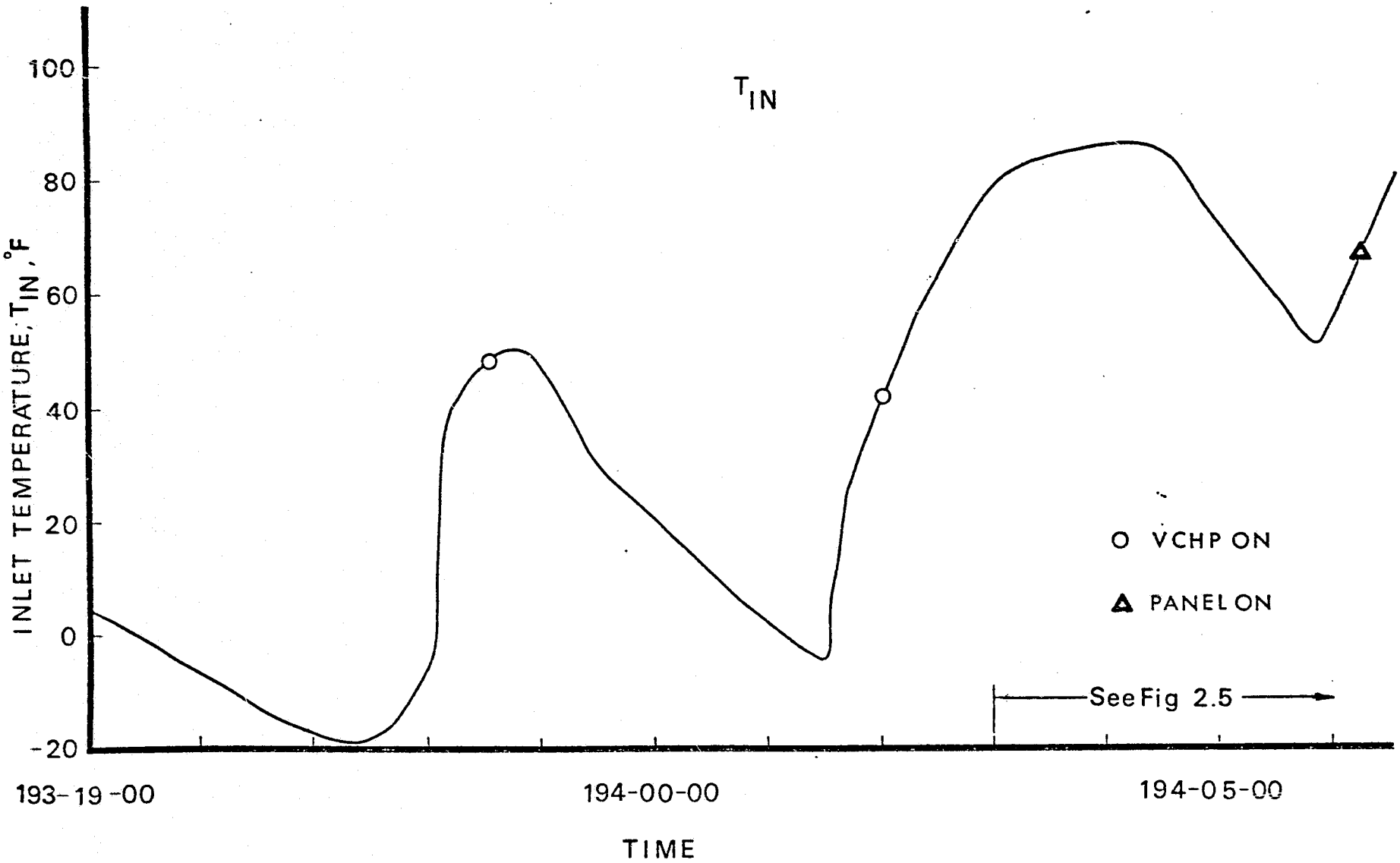

Figure 2.1 Variation of T_{IN} During Thawing

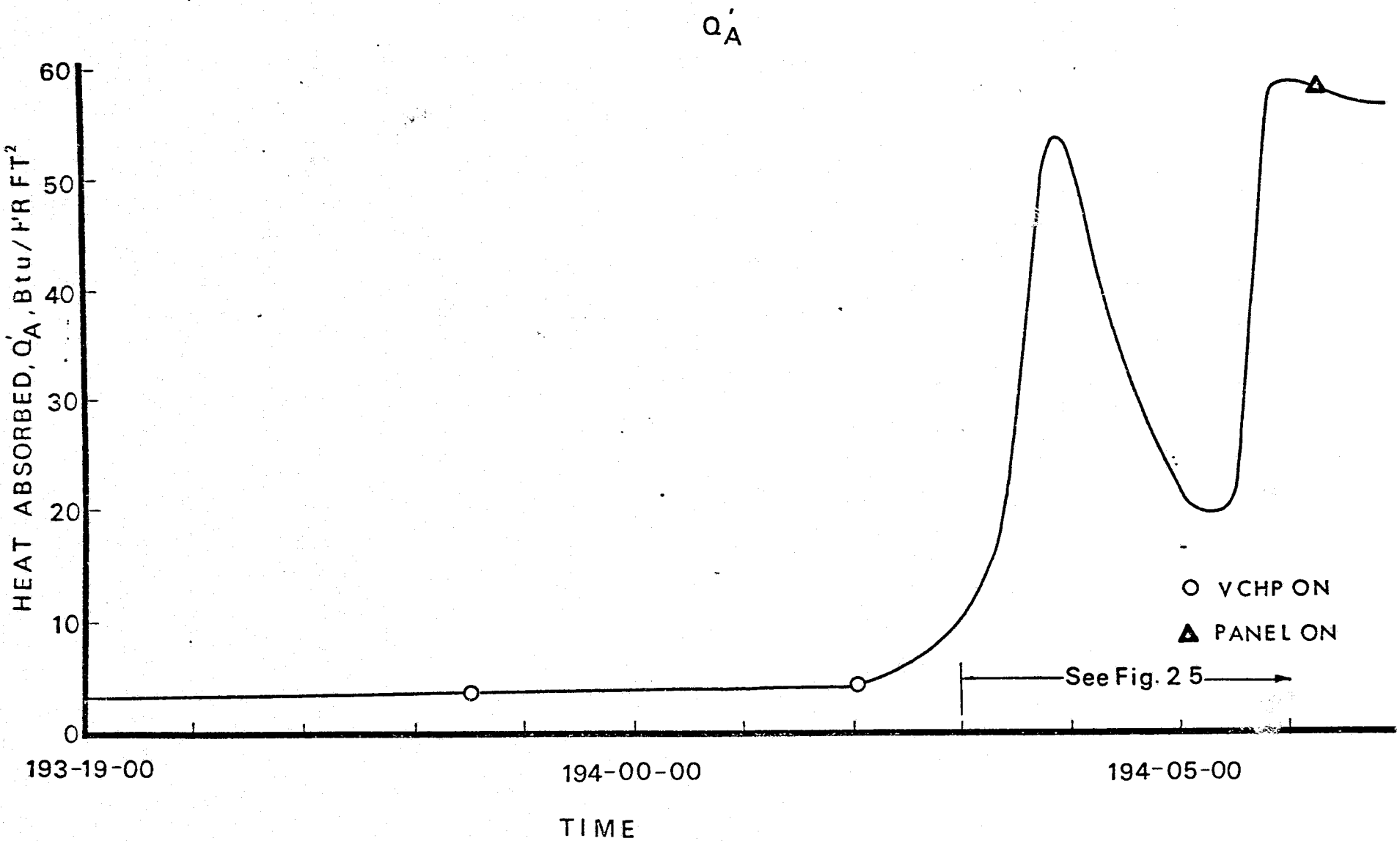

Figure 2.2 Variation of Q'_A During Thawing

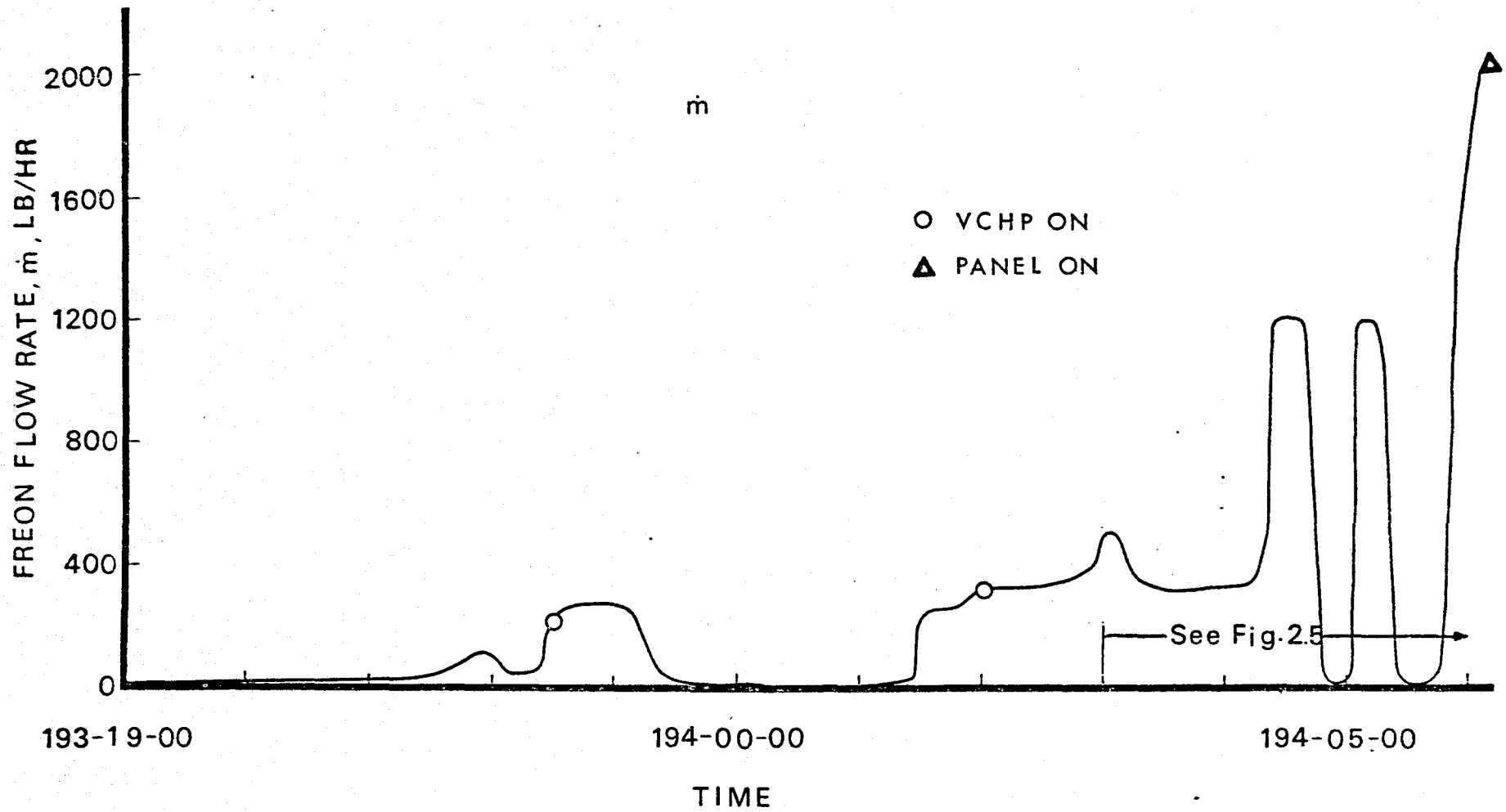

Figure 2.3 Variation of $\dot{m}$ During Thawing

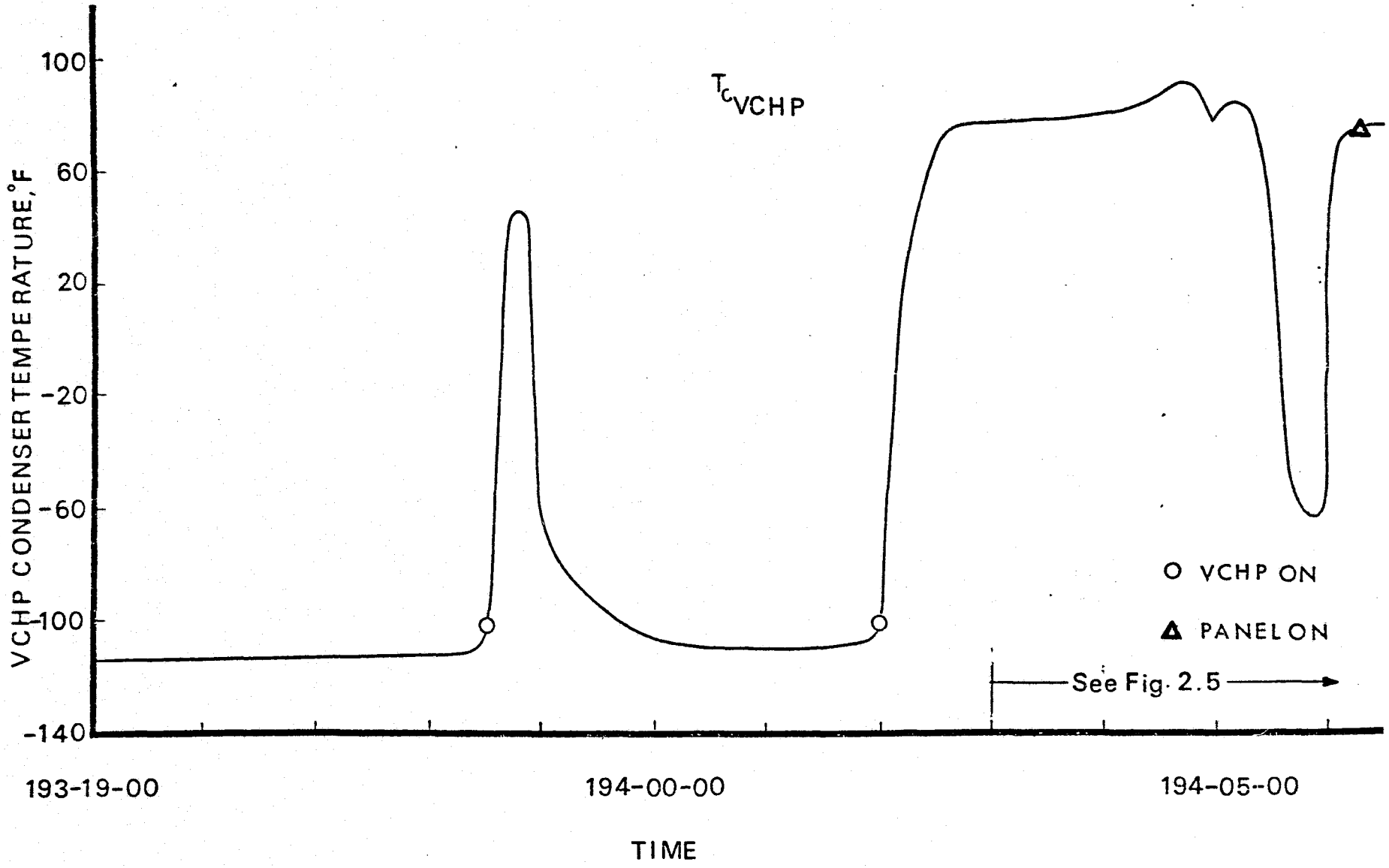

Figure 2.4 Variation of VCHP Header Condenser Temperature During Thawing

As stated above, under these conditions and in the time line of the experiment, the feeder heat pipes had not thawed. Consequently, the Freon inlet temperature was increased from 50 to 83°F. At time 194-03-25, (an hour after the VCHP came on for the second time) and after 13 min. at the higher inlet temperature, the feeders, however, remained frozen, Fig. 2.5.

At this point, the panel environment was increased to a peak value of 55 Btu/hr-ft^2 and then decreased during the next hour (Freon temperature and flow of 83°F and 350 lb/hr, respectively) which resulted in a slight thawing of the feeders, Fig. 2.5, but a study of the panel temperature data indicated they did not begin to heat pipe.

At time 194-04-25, the Freon flow was increased to 1200 lb/hr. The feeders continued thawing, but after a 25 min. waiting period they still had not commenced heat pipe operation. The average environment during this period was 25 Btu/hr-ft^2.

Now, over 2 hours of the experiment had elapsed since thawing conditions had been initiated, and without the panel functioning. At 194-04-50, the operator acting on the supposition that the feeders had not reprimed because of the potential heat load level (recall the VCHP header was functioning) shut off the 83°F Freon flow. After about a 15 min. wait, the flow was resumed at 1200 lb/hr. (Q'_A = 22 Btu/hr-ft^2, T_{IN} = 83°F). At this point in time, the feeders and panel were still not functioning in a normal manner as indicated by their temperatures.

Consequently, the Freon flow was shut off again and in addition

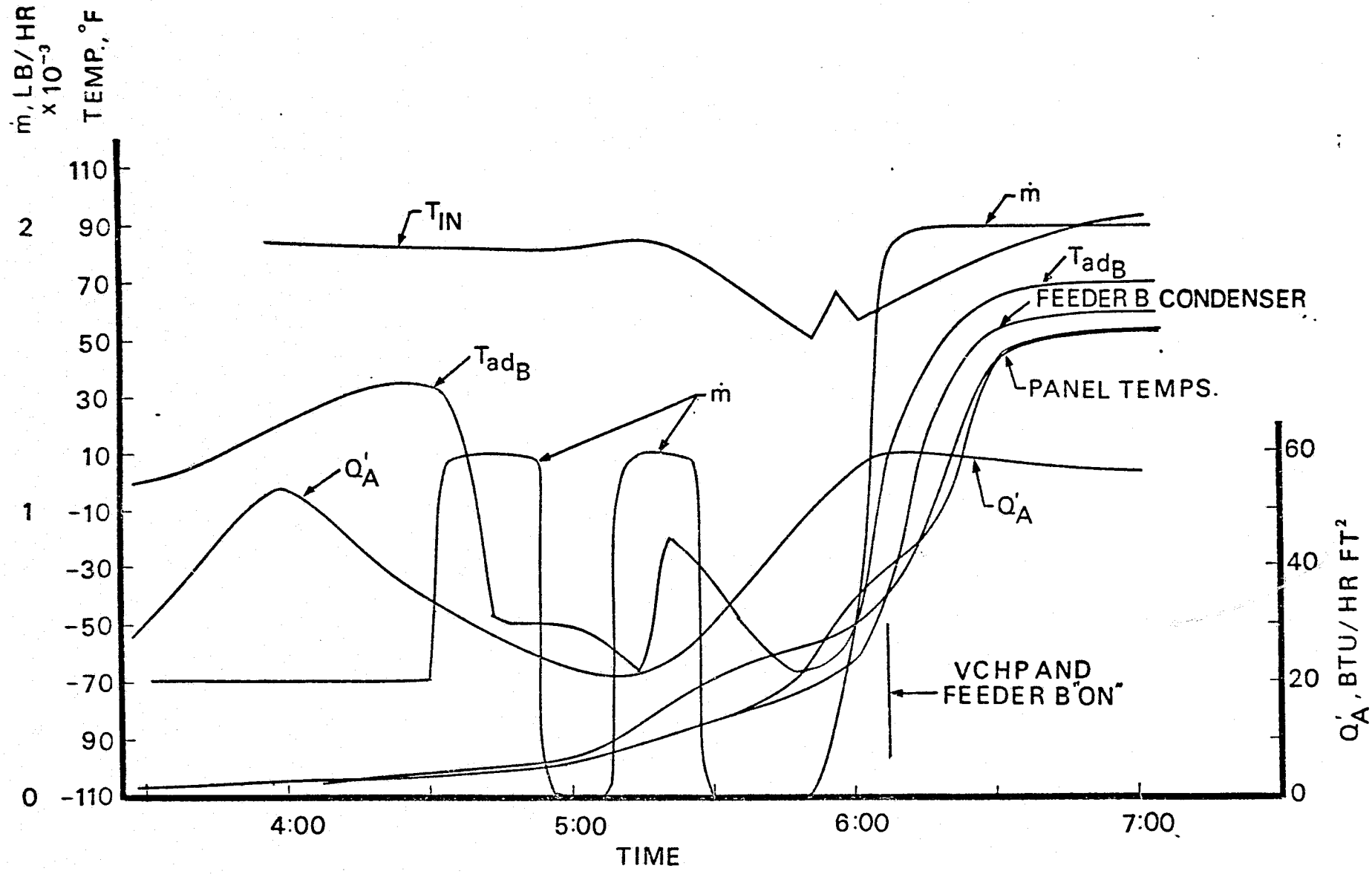

Figure 2.5 Variation of Parameters which Produced Feeder Thawing

the Freon temperature was reduced from 83 to 55°F, which in effect removed any heat load on the feeders by shutting off the VCHP, Fig. 2.5. Unfortunately, and probably inadvertently, at this point Q_A' was increased from 20 to 60 Btu/hr-ft^2. At 194-05-50 the Freon flow had been resumed ($\dot{m}$ = 400 lb/hr and increasing). On this attempt the VCHP header restarted, the feeder heat pipes primed and began functioning between 194-05-55 and 194-06-30 under the following transient conditions:

$$\dot{m} = 0 - 2000 \text{ lb/hr}$$

$$T_{IN} = 55 - 80^\circ F$$

$$Q_A' = 60 \text{ Btu/ft}^2\text{hr}$$

In summary, thawing and restarting the VCHP header from a frozen state presented no difficulty and could be accomplished within an hour. Thawing and restarting of the feeders, although finally successful, was much more arduous. The feeder heat pipes did reprime in the experiment when the VCHP and feeder heat pipes were made to come on nearly simultaneously under thawing conditions. This was accomplished by off-on control of the VCHP. No definite conclusions as to the necessity of such a procedure can be made, however, since a simultaneous increase of the environment from 20 to 60 Btu/hr-ft^2 occured, which may have been the dominating activating factor.

3.0 FEASIBILITY VCHP AMBIENT SUPPLEMENTAL HEATING AND TILT TESTS

The VCHP heat pipe radiator panel when tested in a thermal vacuum chamber at JSC operated successfully only under limited conditions and demonstrated a maximum capacity less than 550 watts, considerably under the level expected, and unacceptable for future applications. Careful analysis (2) of the available data indicated that during the tests, the VCHP header was heat capacity limited. In order to experimentally study the VCHP under more convenient and controllable conditions, and hopefully establish the cause for its limited capacity, a series of ambient tests was made recently at JSC. The main differences in the vacuum and ambient tests were that in the latter (a) convection cooling rather than radiation panel cooling was used and (b) water was substituted for Freon.

Steady state, or near steady state, data points as determined by the data records, Appendix A, for the October 18-24 ambient test series are tabulated in Table 3.1.

Data points 1 thru 4, taken on October 21, 1974, pertain to the movement of the gas-vapor interface in the VCHP toward the reservoir as the water inlet temperature into the heat exchanger is increased from 113°F to 126°F. During the October 23 tests, the coolant inlet temperature was held constant and the reservoir temperature was decreased from 71°F to 24°F, thereby increasing the conductance of the VCHP. The supplemental heating and tilt tests were made the following day.

3.1 Variation of T_{IN}

Data points 1 thru 5 give the effect of T_{IN} on T_V, Q and for a

Data Point	Date	Time	T_{IN} °F	$\dot{m}$ LB/HR	T_R °F	T_{BATH} °F	T_V °F	ΔT °F	Q BTU/HR	Inter-face TC	ψ	REMARKS
1	Oct. 21 1974	1:53	113	.31	55	97	113	.7	102	4	0	VCHP came on.
2	"	3:35	122	.32	70	97	116.5	5.8	964	11+	.38	
3	"	4:13	126	.32	70	96.5	119	7.2	1171	11++	.4	
4	"	6 00	125	.4	67	96.5	118.5	6.2	1243	12	.41	
5	Oct. 23 1974	1:20	115	.33	71	97	114	1.9	314	5	.07	
6	"	2:13	115	.33	63	97	112	3.6	596	9	.26	
7	"	2:40	116	.33	55	96.5	111.5	4.3	711	11+	.36	
8	"	2:57	116.5	.33	54	97	111.5	4.3	711	11+	.38	
9	"	3:34	116	.33	49	97	110.5	4.7	777	12+	.44	
10		4:15	116	.33	37	98	108.5	5.6	926	17+	.7	
11	"	4:40	116	.33	31	98	107.5	6.0	1002	20+	.87	
12	"	5:15	116	.33	24	98	107	6.1	1018	21+	.94	
13		1:55	90	32	28	70.5	90	.2	30	4	0	VCHP came on.
14	Oct.24 1974	3:40	105	.34	29	70	98	6.7	1142	10++	.34	Before supplemental heating.
15	"	3:50	105	.35	31	71.5	101	5.5	937	12+	.44	With supplemental heating. Q is for heat exchanger only.
16	"	6:20	105	.32	27	69.5	95	9.3	1492	12+	.44	Before positive tilt.
17	"	6:40	105	.32	28	66	95	10	1604	15+	.6	With 1/2" positive tilt.

Table 3.1 Ambient Supplemental Heating and Tilt Test Data

variation of T_{IN} from 113 to 126.5°F, T_R and $\dot{m}$ near constant. The experimental association between T_V and ϕ is presented in Fig. 3.1. Also presented in Fig. 3.1, for comparison, are calculated curves and earlier vacuum chamber data (2).

Referring to the ambient tests (upper curves in Fig. 3.1), it can be seen that as the VCHP came on, Test 1, and as ϕ increased Tests 2, 3, 4, and 5, due to higher heat exchanger inlet temperatures, the experimental vapor temperatures did not follow the calculated curves, but fall above them. The thermal vacuum tests, Fig. 3.1, had shown a similar trend. It can also be seen that in the vacuum tests the VCHP opened at a slightly lower vapor temperature than predicted, but in the ambient tests the reverse occured. In general, however, the overall results are similar for both the ambient and vacuum VCHP test series.

The calculated curves in Fig. 3.1 were obtained from the VCHP control equation (1):

$$\varphi = 1 + (V_R/V_C)(T_S/T_R)(P_V - P_{V_R})/(P_V - P_{V_S}) - m_g R_g T_S/V_C(P_V - P_{V_S}) \qquad 3\text{-}1$$

3.2 Variation of T_R

In Sec. 3.1, the inert gas interface in the VCHP was made to recede toward the reservoir by elevating the heat exchanger inlet fluid temperature. From Eq. 3.1, it can be seen that a similar result can be obtained by a lowering of the temperature level of the reservoir.

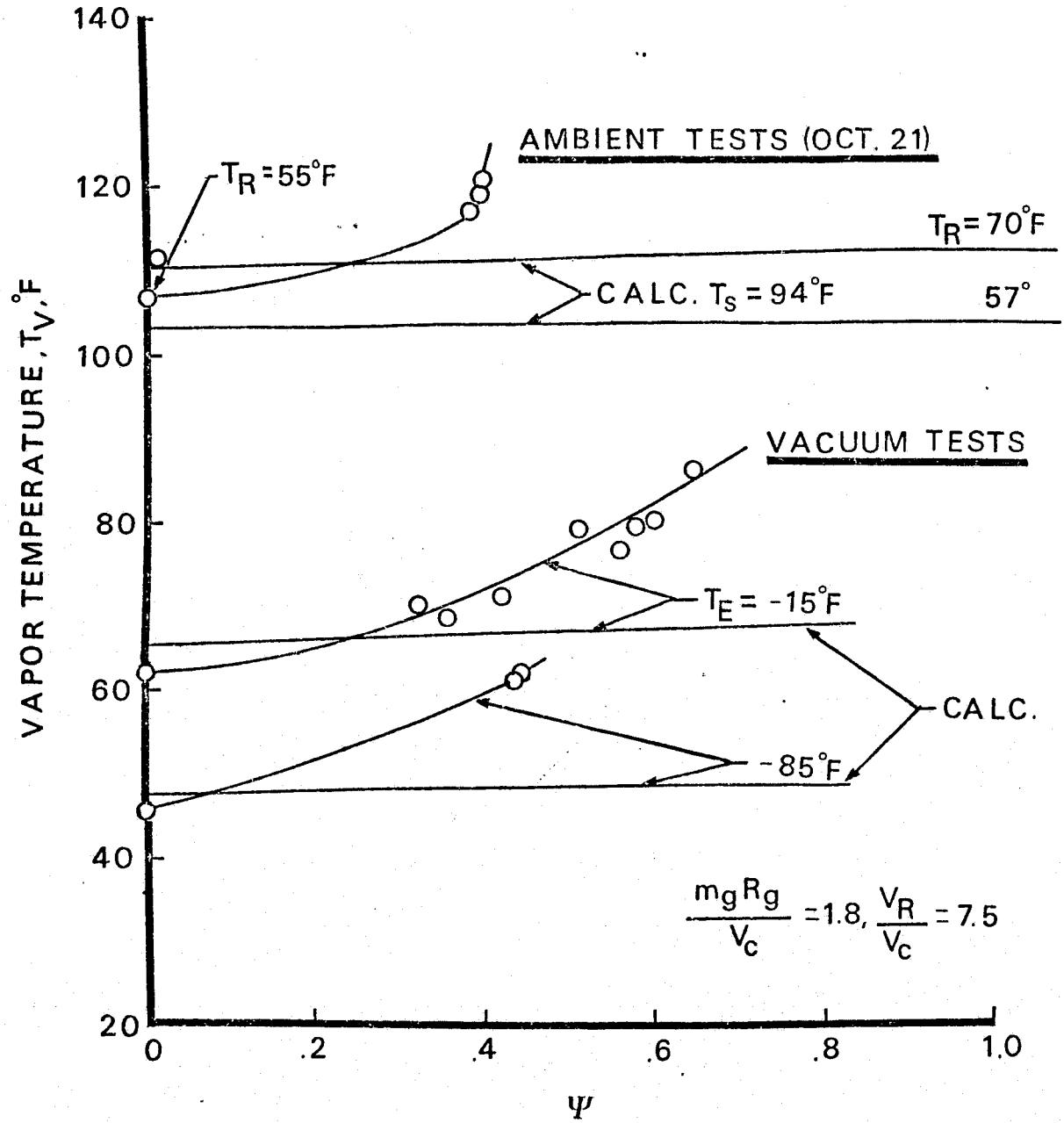

Figure 3.1 T_V and ϕ Values when T_{IN} was Varied in Ambient Tests

Data points 5 thru 12, Table 3.1, give the effect of T_R on ϕ T_V, Q and for a variation of T_R from 24 to 71°F, T_{IN} and $\dot{m}$ nearly constant. Refer to Fig. 3.2. Note that the calculated results fall in a band, since at a given reservoir temperature there is a small calculated variation of T_V as ϕ varies from 0 to 1.0. It is interesting to note that the VCHP was over 90% open at a reservoir temperature of 24°F (T_{IN} = 116°F), but the heat transport capacity was not high, due to the relatively low heat-exchanger inlet temperature. Comment: With the interface established at ϕ = .94, as in data point 12, it perhaps would have been informative if the inlet temperature had then been increased to determine maximum Q. The value obtained could then be compared with the maximum value observed in the vacuum tests and also the calculated VCHP design performance figure.

Referring to Fig. 3.2, it is apparant that at a given reservoir temperature the experimental vapor temperature is considerably higher than theoretical. The difference between the experimental and calculated curves is greatest at the lower reservoir temperature where the VCHP is most open and the heat transport is maximum.

3.3 Supplemental Heating (S.H.)

The S.H. tests were conducted on October 24, 1974. A study of data points 14 and 15 helps to bring out the effect of S.H. on the VCHP performance. Conditions immediately prior to S.H. correspond to data point 14. A comparison of the T_V, ϕ values obtained when S.H. was applied near the heat exchanger end of the VCHP condenser, data point 15, to the T_V, values of data point 14 are presented in Fig. 3.3. It is evident that S.H. resulted in an

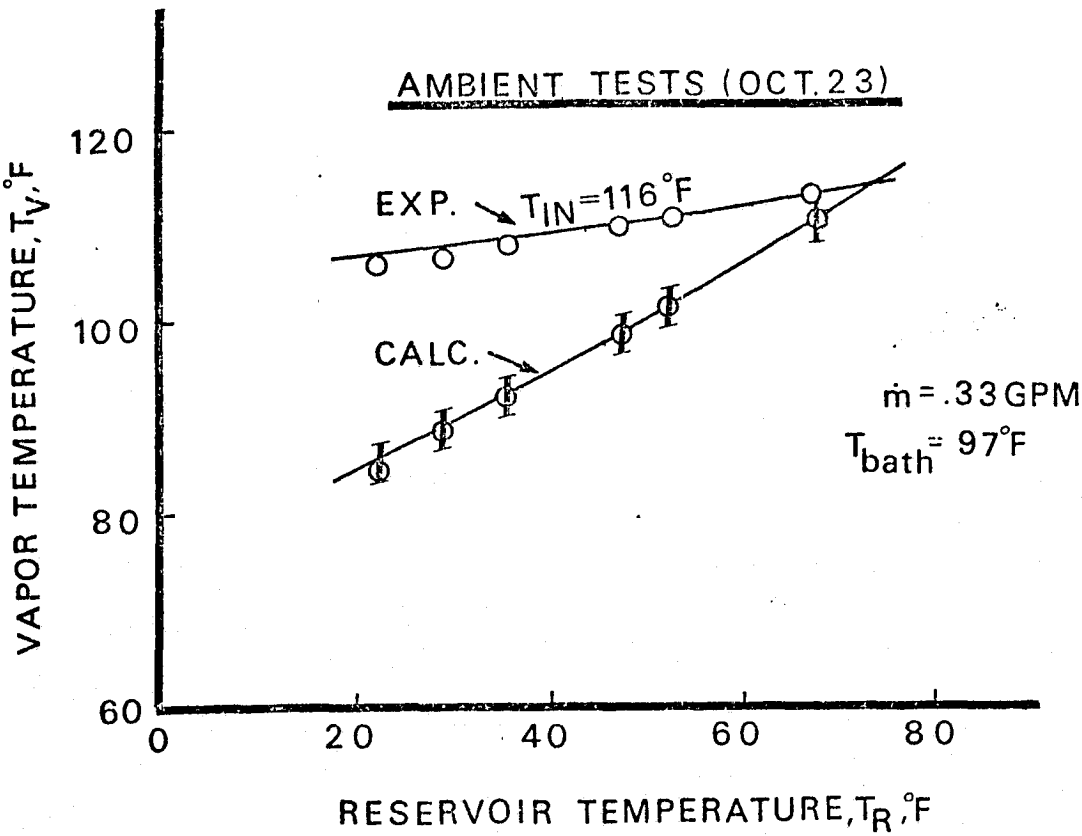

FIG.3.2 Comparison of ambient tests with analysis; T_R variation.

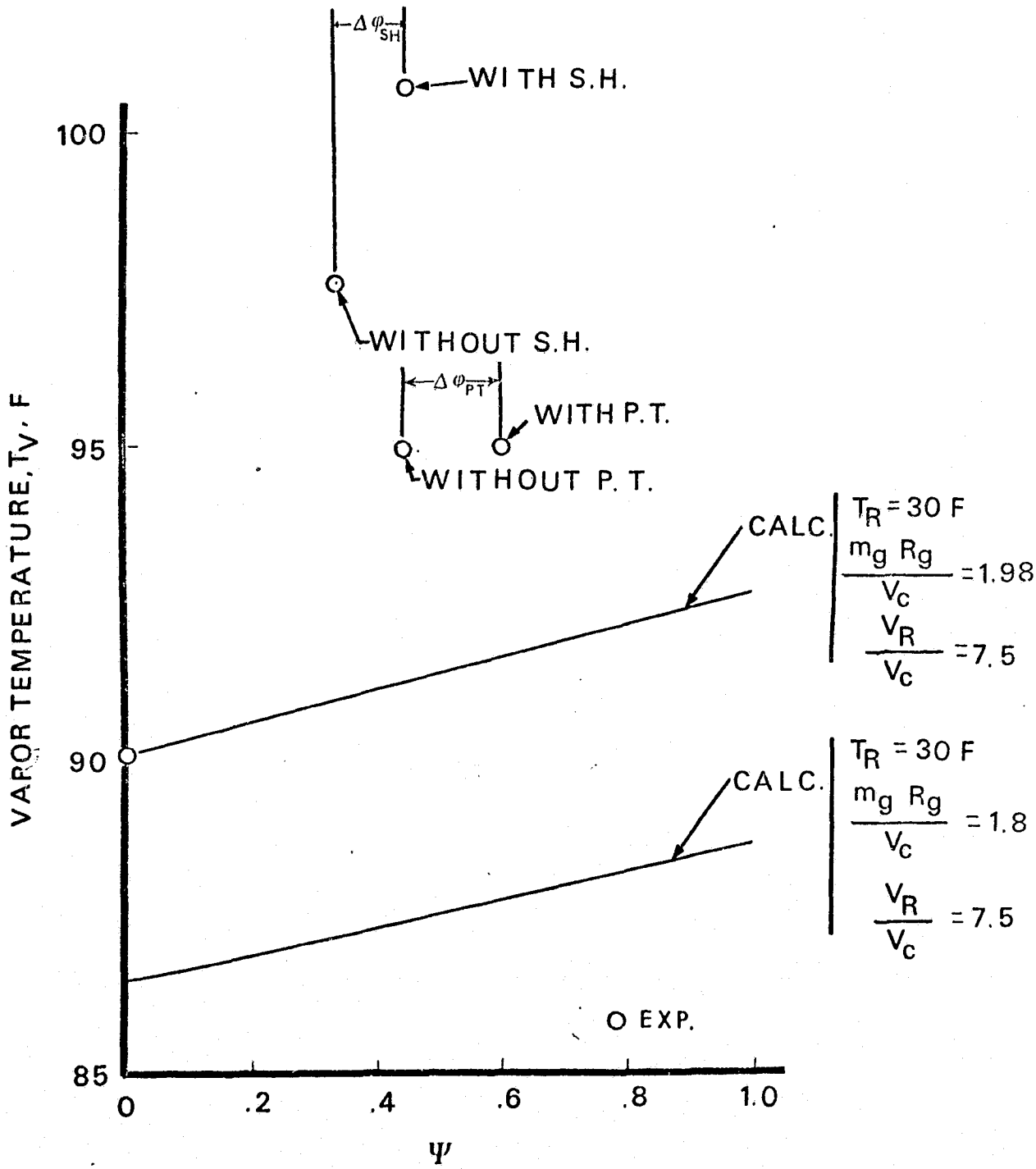

Figure 3.3 Comparison of Supplemental Heating and Positive Titlt Results

increase in ϕ from .34 to .44, or 29%, and T_V rose to 101°F from 97.5°F. The heat transfer in the heat exchanger decreased from 1142 Btu/hr to 937 Btu/hr presumably due to the increase of T_V. The increase of ϕ, however, may be misleading, since a portion of the VCHP condenser area became part of the evaporator when the supplemental heating was applied, and was not considered in the calculation of the 29% value.

Comment: It is interesting to compare the October 24th data with earlier results. The inlet temperature T_{IN} for data point 14 is 11 degrees lower than that of data point 11, taken one day earlier, but the heat transfer is higher, 1142 Btu/hr compared to 1002 Btu/hr. The increase in heat transfer is believed partly due to a 28°F lower bath or sink temperature for data point 14, and possibly experimental inaccuracies.

3.4 Positive Tilt (P.T.)

Approximately three hours after the supplemental heating experiments, a positive tilt (header condenser elevated above header evaporator) was applied to the feasibility VCHP. Data point 16 occurred 20 minutes before the VCHP header was tilted, and data point 17 are the results of a 1/2 in positive tilt. The T_V, ϕ values for both conditions are shown with the S.H. results in Fig. 3.3. The effect of P.T. was to increase ϕ from .44 to .6, 36%, with no increase, or reduction, in T_V.

Included in Fig. 3.3 are calculated values of T_V vs. ϕ from Eq. 3-1 for two values of $m_g R_g/V_c$, 1.8 and 1.98 lb/in^2°R. The latter value was used to give agreement with the experimental value

of T_V obtained from data point 13. Of the four experimental points, including supplemental heating, where $\phi > 0$ in Fig. 3.3, the best agreement with the calculated curve was the P.T. data.

Comment: After the supplemental heating and prior to the positive tilt experiments the performance of the VCHP panel appeared to improve for no obvious reason. For example, the VCHP heat output was 30% higher for data point 16 compared to data point 14, although their operating conditions were nearly identical. The 3 degree lower reservoir temperature that occurred in data point 16 could account for some increase in heat transfer, but not a 30% increase.

3.5 Summary

The ambient VCHP test data when compared with analysis are similar to the vacuum test results; that is, the increase of vapor temperatures is more than predicted with accompanying small changes in ϕ as the heat exchanger inlet temperature was increased. The difference between experimental and calculated results is directly proportional to the heat transport.

The effect on the VCHP performance when supplemental heating and positive tilt was applied was similar in that both produced some movement of the gas vapor interface toward the reservoir. With supplemental heating, however, the vapor temperature increased which reduced the normal heat transfer in the heat exchanger, and resulted in greater deviation from theoretical than before supplemental heating.

The effect of a ½ in. positive tilt resulted in slightly better agreement with theoretical than before a positive tilt. It may be conjectured that even closer agreement with theoretical may have been

obtained if the heat load had been reduced prior to the positive tilt in order to provide more favorable conditions for wick priming.

4.0 ANALYSIS OF FLUID HEADER HEAT PIPE RADIATOR

4.1 Equations

The fluid header heat pipe radiator system is physically and analytically similar to the VCHP feasibility panel analyzed in reference (1) as both have a selected number of heat pipes attached to a radiator. Refer to Fig. 4.1. In the case of the fluid header, the evaporator ends of these heat pipes (feeders) are emmersed axially in the header tube through which the Freon coolant flows. Heat is transferred from the Freon to the feeders and then transported to the radiator where it is radiated to space.

The following equations (1) describe the system:

$$Q_{REJ} = \dot{m} C_p (T_{IN} - T_{OUT})$$

$$Q_{REJ_i} = Q_{REJ} / N_p \quad \text{(For first iteration only)}$$

$$i = 1, 2, 3 \cdots N_p$$

$$Q_{REJ_i} / \dot{m} C_p = (T_{IN} - T_{OUT})$$

$$T_{IN_i} = T_{OUT_{i-1}}$$

$$Q_{REJ_i} / C1 = (T_{IN_i} - T_{OUT_i}) / \ln \left[\frac{T_{IN_i} - T_{V_i}}{T_{OUT} - T_{V_i}} \right]$$

$$1/C1 = R_1 + R_2$$

$$R_1 = 1 / h_o A_o \eta_o$$

$$R_2 = 1 / h_5 \pi D_{ihp} L_{ehp}$$

$$T_{V_l} - T_{n_{R_i}} = Q_{RE} J_i / C2$$

$$1/C2 = R_6 + R_7$$

$$1/R_6 = h_6 \pi D_{i_{hp}}/2) L_{c_{hp}} n_6$$

$$1/R_7 = h_7 L_{c_{hp}} (w_7/2)$$

$$h_o = \begin{cases} 1.86(k_l/D_h)(R_e Pr)^{1/3}\left(\dfrac{D_h}{L_{e_{hp}}/2}\right)^{1/3} & R_e < 2300 \\ .023(k_l/D_h) R_e^{.8} Pr^{1/3} & R_e \geqq 2300 \end{cases}$$

$$R_e = D_h \dot{m} / \mu_l A_c$$

$$Pr = (C_p \mu / k)_l$$

$$A_c = \beta D_h \pi (D_{i_{hx}}^2 - D_{hp}^2)/4$$

$$A = \beta L_{e_{hp}} \pi (D_{i_{hx}}^2 - D_{hp}^2)/4$$

$$n = 1 - (1 - n_f)(A_f/A_o)$$

$$n_f = \left(\tan h (mb)\right) \div (mb)$$

$$m = (2h_o/k\delta)^{1/2}$$

$$b = (D_{i_{hp}} - D_{o_{hp}})/2$$

Nodal points are spaced evenly along the midline of the panel and perpendicular to the feeders as shown in Fig. 4.1, and for each node a finite difference equation is written. Consider the heat balance for an area L_{chp} x L_n on the panel as shown in Fig. 4.1. Assuming steady state,

$$\text{Heat Input} = \text{Heat Output}$$

$$Q_{n_i} + \frac{K_R L_{chp} t}{L_n}\left[T_{(n-1)_i} - T_{n_i}\right] = L_{chp} L_n\left[h_R(T_{n_i} - T_E') + h(T_{n_i} - T_E\right] + \frac{K L_{chp} t}{L_n}\left[T_{n_i} - T_{(n+1)_i}\right] \qquad n = 1,2,3 \cdots N$$

where

$$h_R = .1714\,\epsilon\left[(T_{n_i}/100)^4 - (T_E'/100)^4\right] \div (T_{n_i} - T_E')$$

$$T_E' = (Q_A'/\alpha\epsilon)^{1/4}$$

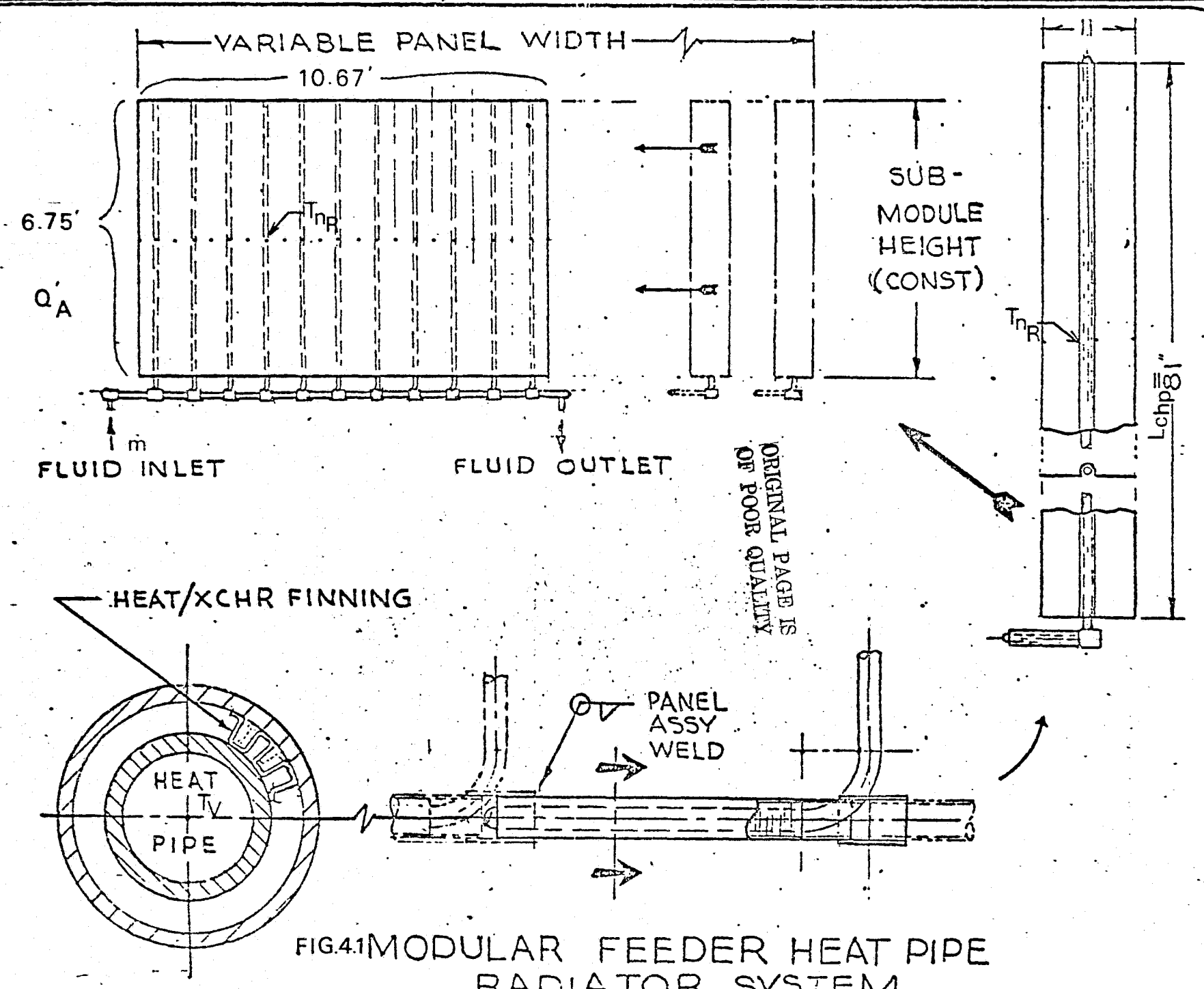

FIG.4.1 MODULAR FEEDER HEAT PIPE RADIATOR SYSTEM

Also, for nodal points not on the feeder heat pipes

$$Q_{ni} = 0.$$

A computer program (Appendix C) containing the above equations was written. The main program output is the heat rejection of the panel for different Freon flow conditions and panel environments.

4.1.1 Single Panel Computer Results

Computer results, Fig. 4.2, were obtained for the prototype radiator panel, Table 4.1, designed and built by Grumman. It can be seen that the 68 ft^2 prototype panel is capable of high heat rejection, particularly at the higher Freon temperatures. Computer results, Table 4.2, were also obtained for a finned fluid header conforming to the original feasibility VCHP header geometry. Thus, it can be seen that the transport capacity for the finned fluid header is 8% higher than the correctly functioning VCHP header and would be 50% higher than the experimentally measured value. A correctly functioning VCHP, of course, has the advantage of self-regulation.

4.1.2 Multiple Panel Computer Results

A multi-panel comparison of the finned fluid header and a VCHP for the feasibility panel configuration was completed for the following panel arrangements:

a. Series

b. Parallel

c. Two parallel branches

d. Three parallel branches

e. Four parallel branches

The results of the computer calculations are shown in Table 4.3.

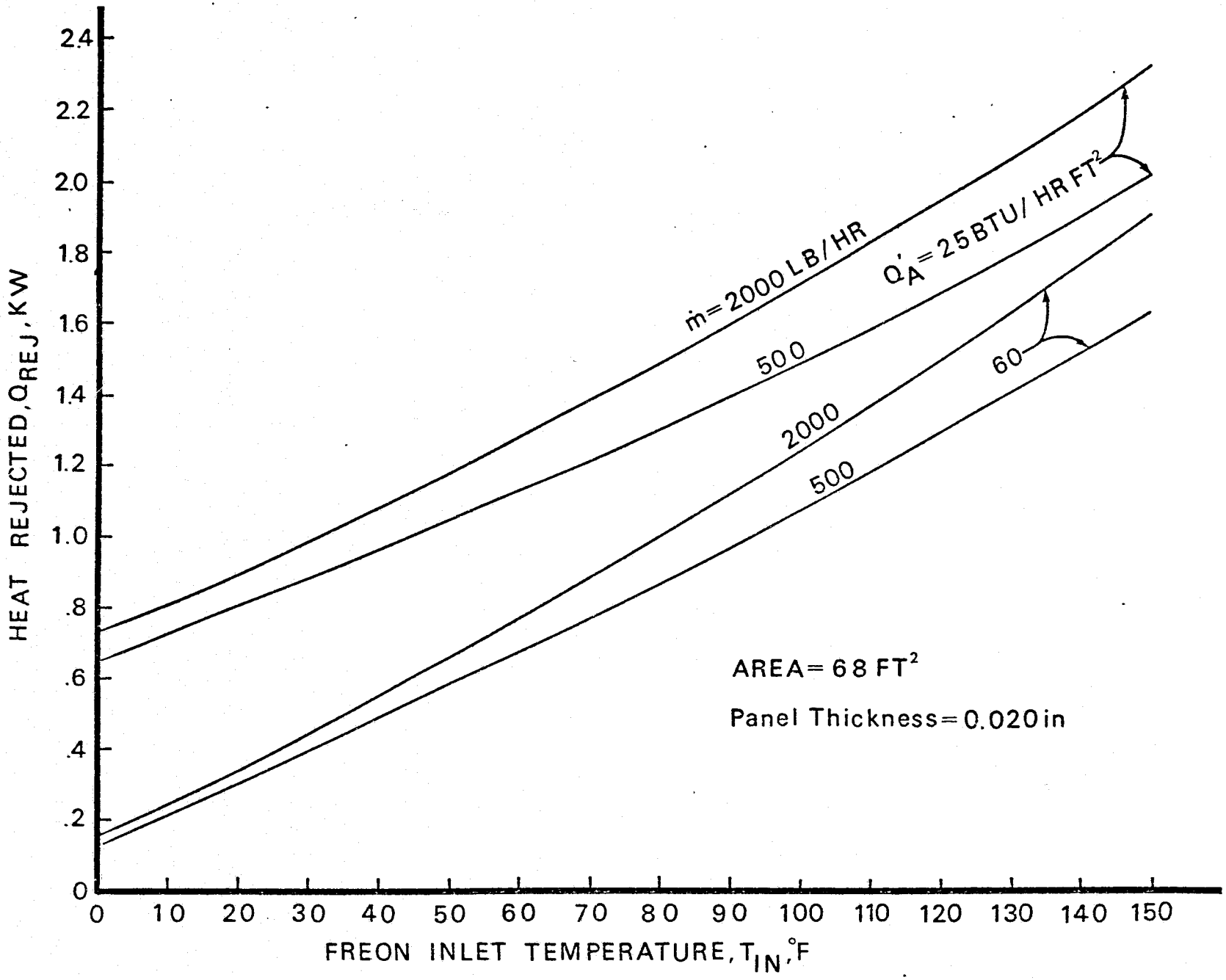

Figure 4.2 Variation of Q_{REJ} with T_{IN} for Two Coolant Flows and Two Environments

	Prototype	Feasibility VCHP
Heat Pipes		
Number	11	6
Working Fluid	Ammonia	Ammonia
Material	6061-T6	6061-T6
OD, in	.625	.625
ID, in	.500	.500
Wick	spiral artery	spiral artery
Heat Exchanger		
Length, in	9 (per heat pipe)	24
Number of fins/in	15	15
Annulus, in	.138	.125
Radiating Fin		
Material	6061-T6	6061-T6
Thickness, in	.020	.020
Width, in	11	8
Length, in	81	96
Effective Area, ft^2	6.19	5.33
Overall Panel		
Heigth, in	81	96
Width, in	128	48
Weight, lb	64	36
Area, ft^2	74.3	32
Weight/Area	.86	1.13

Table 4.1 Prototype Fluid Header Panel and Feasibility VCHP Header Panel

	VCHP	Finned Fluid Header
Q_{REJ} (calc.), watts	537	580
Q_{REJ} (exp.), watts	386	---
Q/A watts/ft^2	17.5	20

Conditions:

(1) Feasibility panel configuration

(2) $T_{IN} = 96^{o}F$

(3) $\dot{m} = 1{,}990$ lb/hr

(4) $Q''_A = 60$ Btu/hr-ft^2

Table 4.2 Comparison of a finned fluid header and a VCHP Header.

	VCHP HEADER (FEASIBILITY PANEL)			FLUID HEADER (FEASIBILITY PANEL)				
	SERIES	PARALLEL	TWO PARALLEL BRANCHES	SERIES	PARALLEL	TWO PARALLEL BRANCHES	THREE PARALLEL BRANCHES	FOUR PARALLEL BRANCHES
TOTAL HEAT REJECTED Q_{REJ}, $\frac{BTU}{HR}$	47,836	47,290	48,199	48,398	48,145	48,153	48,433	49,251
NUMBER OF PANELS, N	29	49	30	26	29	26	27	28
TOTAL SURFACE AREA A, FT^2	899	1,519	930	806	899	806	837	868
AVERAGE ROOT TEMP. T_{nR}, ^oF	70	38	69	75	70	75	74.5	74
T_{IN}, ^oF	150	150	150	150	150	150	150	150
T_{OUT}, ^oF	47	48	46	45	46	46	45	43.5
$\frac{Q}{A}$, $\frac{WATTS}{FT^2}$	15.7	9.2	15.2	17.7	15.8	17.6	17.0	16.7
IMPROVEMENT % FLUID HEADER over VCHP	---	---	---	12.5	71	16	---	---

Table 4.3 Multi-panel Comparisons

For the all-series arrangements, the finned fluid header is expected to give a 13% increase of Q/A over a VCHP. For the all-parallel case, the Q_{REJ} for a finned fluid header is 71% above the all-parallel VCHP header panels. This latter improvement is the result of a much higher average root temperature for the fluid headers compared to the VCHP headers, 75°F and 38°F, respectively.

Note also that the Q/A difference between the all-series and all-parallel fluid header arrangement is only 12%.

4.2 Parametric Study

A parametric study of a fluid header heat pipe radiator, conforming to the prototype geometry of Table 4.1, was made by varying the values of different design parameters in the computer program (Appendix C), and studying the system's heat rejection.

4.2.1 Thermal conductivity of the radiator panel, K_R.

Figure 4.3 shows the effect of variation in thermal conductivity of the radiator panel on Q_{REJ} for two different environments. An increase in the nominal value from 95 to 150 Btu/hr ft °F would result in an increase in Q_{REJ} of 5.2 percent for an environment of 60 Btu/hr ft^2 and 6.8% for an environment of 25 Btu/hr ft^2.

4.2.2 Thermal conductivity of the heat exchanger fin material, k.

Figure 4.4 brings out that a variation of k from 25 to 150 Btu/hr-ft-°F had no appreciable effect on Q_{REJ}.

4.2.3 Evaporator length of feeder heat pipes, Le_{hp}.

Referring to Fig. 4.5, it can be seen that increasing Le_{hp} from 0.5 to 0.8 ft increases the value of Q_{REJ} by 3 percent and further length increases have negligible effect.

4.2.4 Contact width between feeder heat pipes and panel, w_7.

Figure 4.6 shows the effect on Q_{REJ} when w_7 is changed. An increase

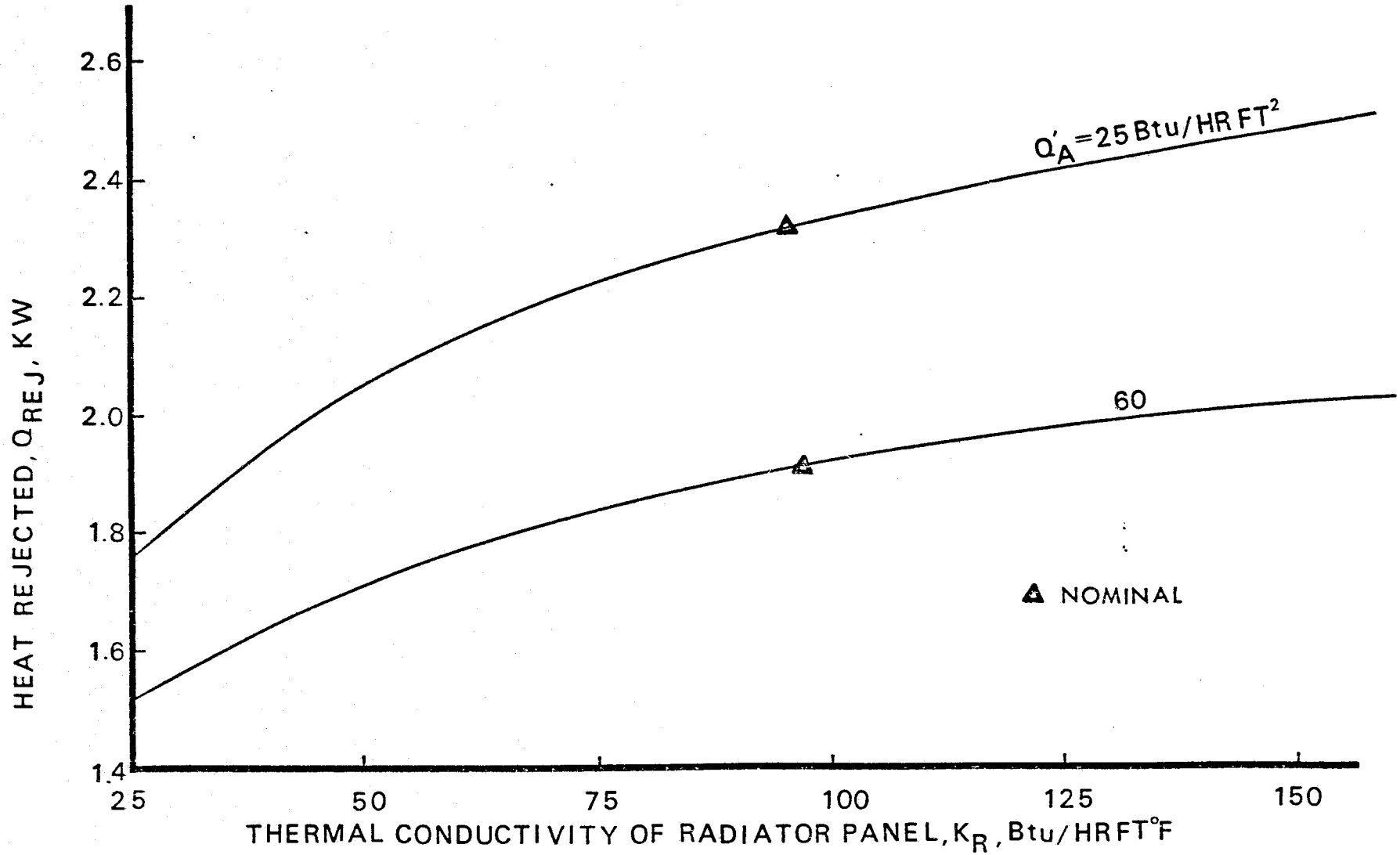

Figure 4.3 Q_{REJ} vs Radiator Panel Thermal Conductivity

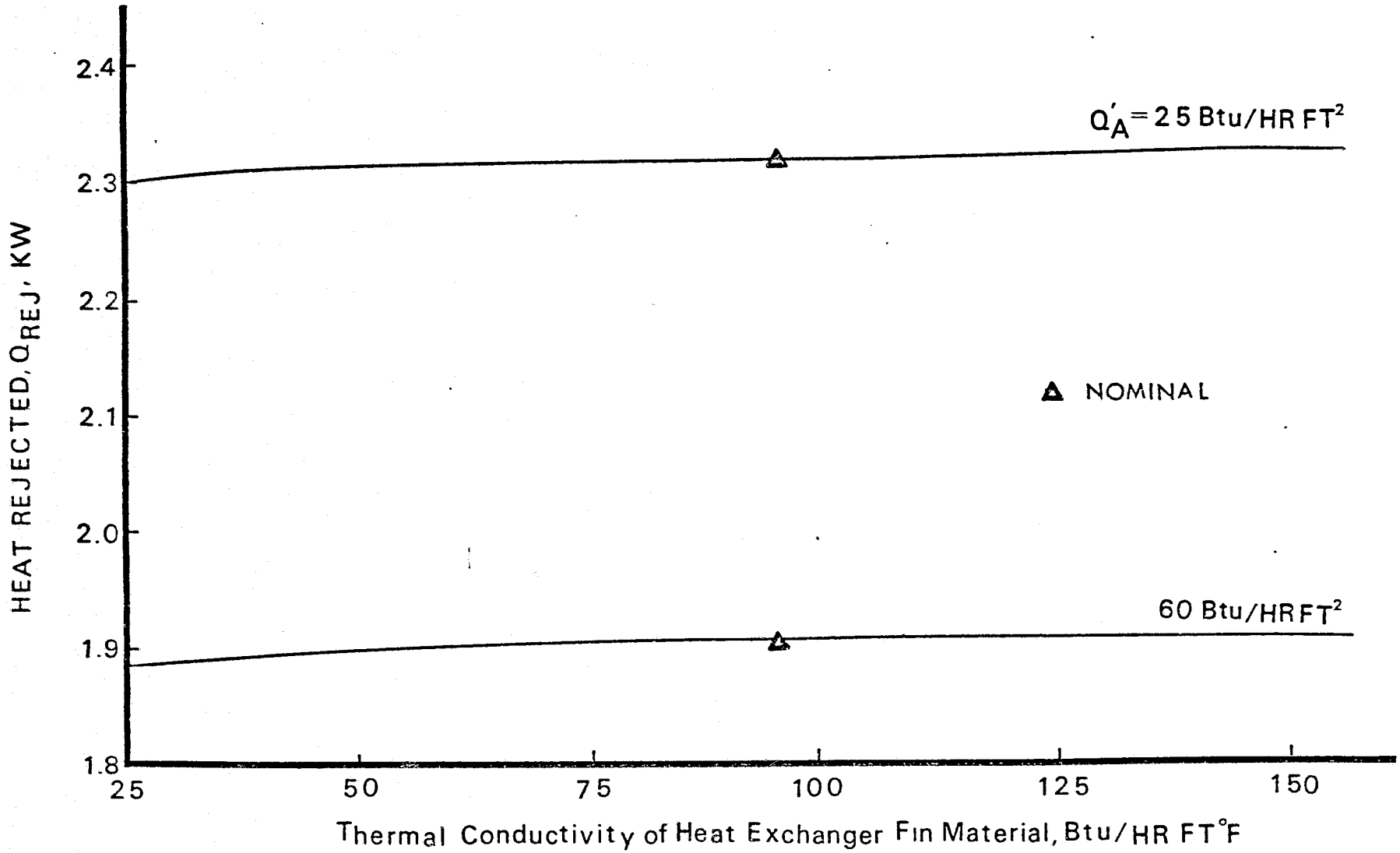

Figure 4.4 Q_{REJ} vs Thermal Conductivity of Evaporator Fins

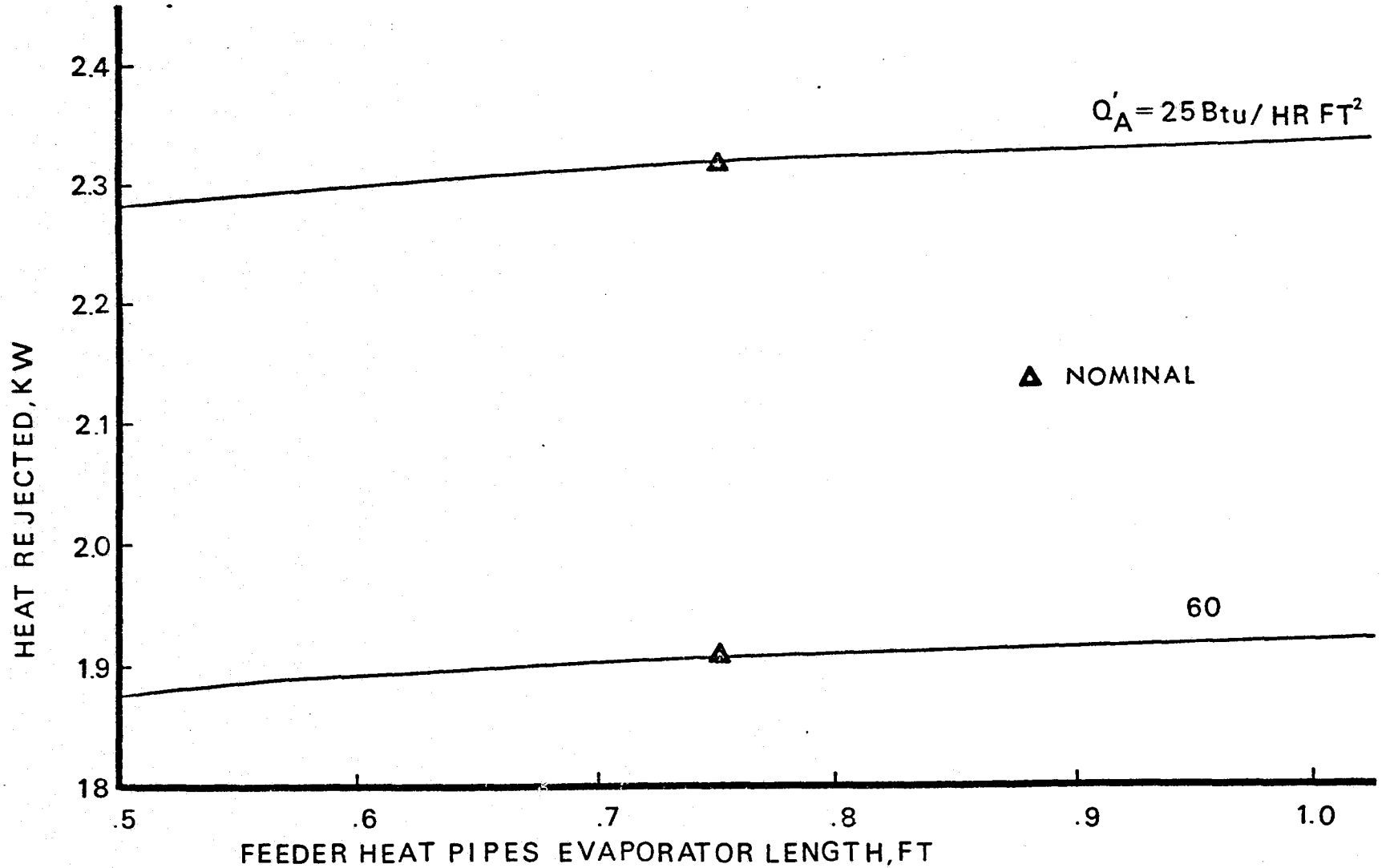

Figure 4.5 Q_{REJ} vs Heat Pipe Evaporator Length

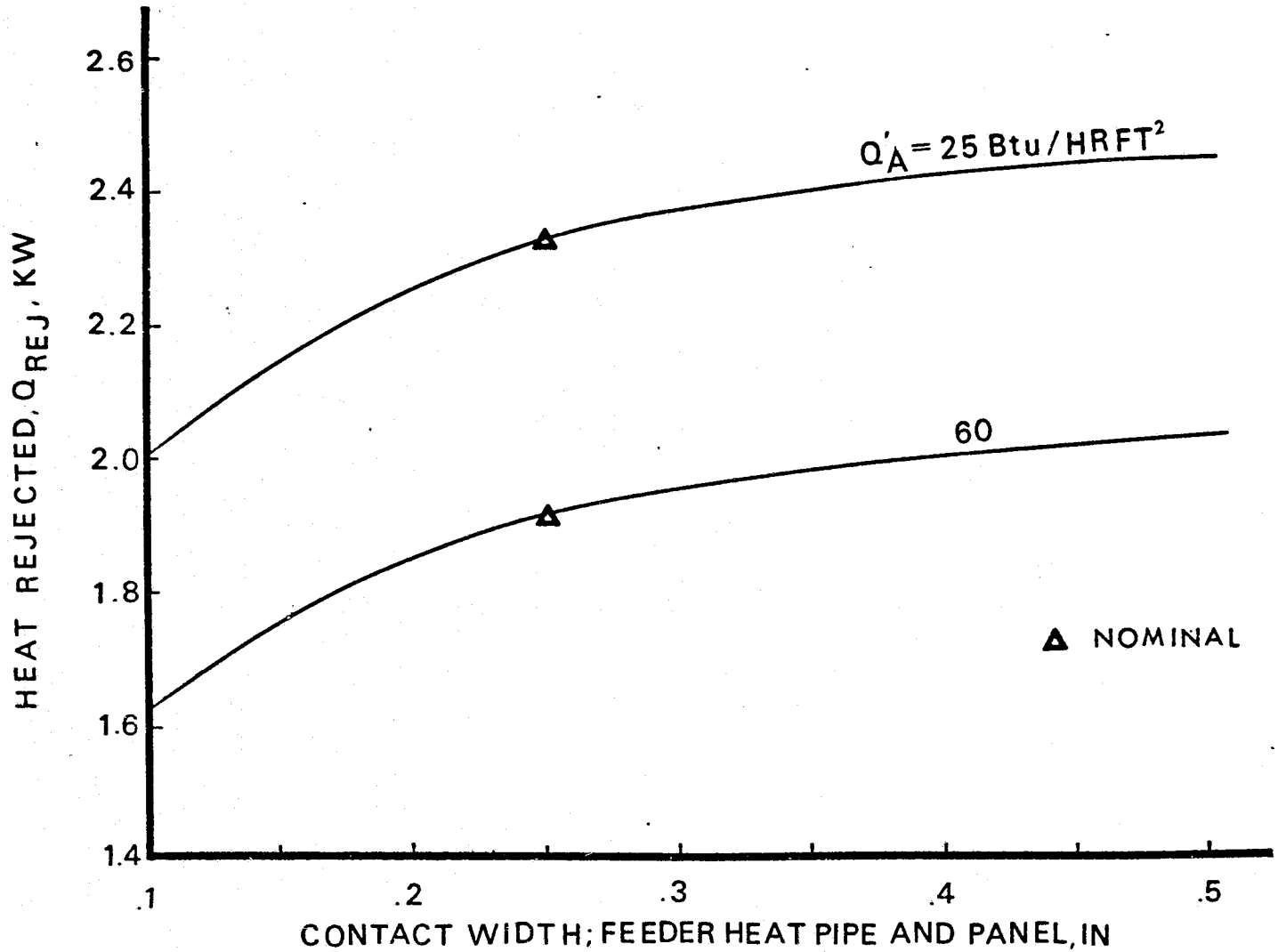

Figure 4.6 Q_{REJ} vs Panel-Heat Pipe Contact Width

of the nominal value from 0.25 in. to 0.4 in. raises the value of Q_{REJ} significantly.

4.2.5 Feeder heat pipe evaporation heat transfer coefficient, h_5.

Q_{REJ} versus h_5 is presented in Figure 4.7. It is evident that h_5 should be above 1000 Btu/hr-ft^2-^{o}F, but beyond that value there is only a small gain of Q_{REJ}.

4.2.6 Feeder heat pipe condenser heat transfer coefficient, h_6.

From Fig. 4.8, it is evident that any increase in the nominal value of h_6 has negligible effect on Q_{REJ}, and in fact the nominal value of 3,000 Btu/hr-ft^2-^{o}F could be reduced by a factor of at least 3 without a large drop of Q_{REJ}.

4.2.7 Contact heat transfer coefficient between heat pipe and panel, h_7.

Figure 4.9 shows that an increase of h_7 from 200 to 800 Btu/hr-ft^2-^{o}F improves Q_{REJ} by 22 percent. Beyond 800 Btu/hr-ft^2-^{o}F the gain in Q_{REJ} is small, or negligible.

4.2.8 Thickness of radiator panel fins, t.

It is seen from Fig. 4.10 that Q_{REJ} increases with increasing thickness of the radiator panel. From Q_{REJ} considerations only, neglecting weight, it would be desirable to increase the thickness of the radiator panel fins.

4.3 Optimum Heat Pipe Spacing

An optimization study was conducted to determine the heat rejection for the fluid-header panel divided by the panel weight, Q_{REJ}/W, versus feeder heat pipe spacing, S, for various panel thicknesses and various panel dimensions.

In the first case, a rectangular panel of 70 ft^2 surface area

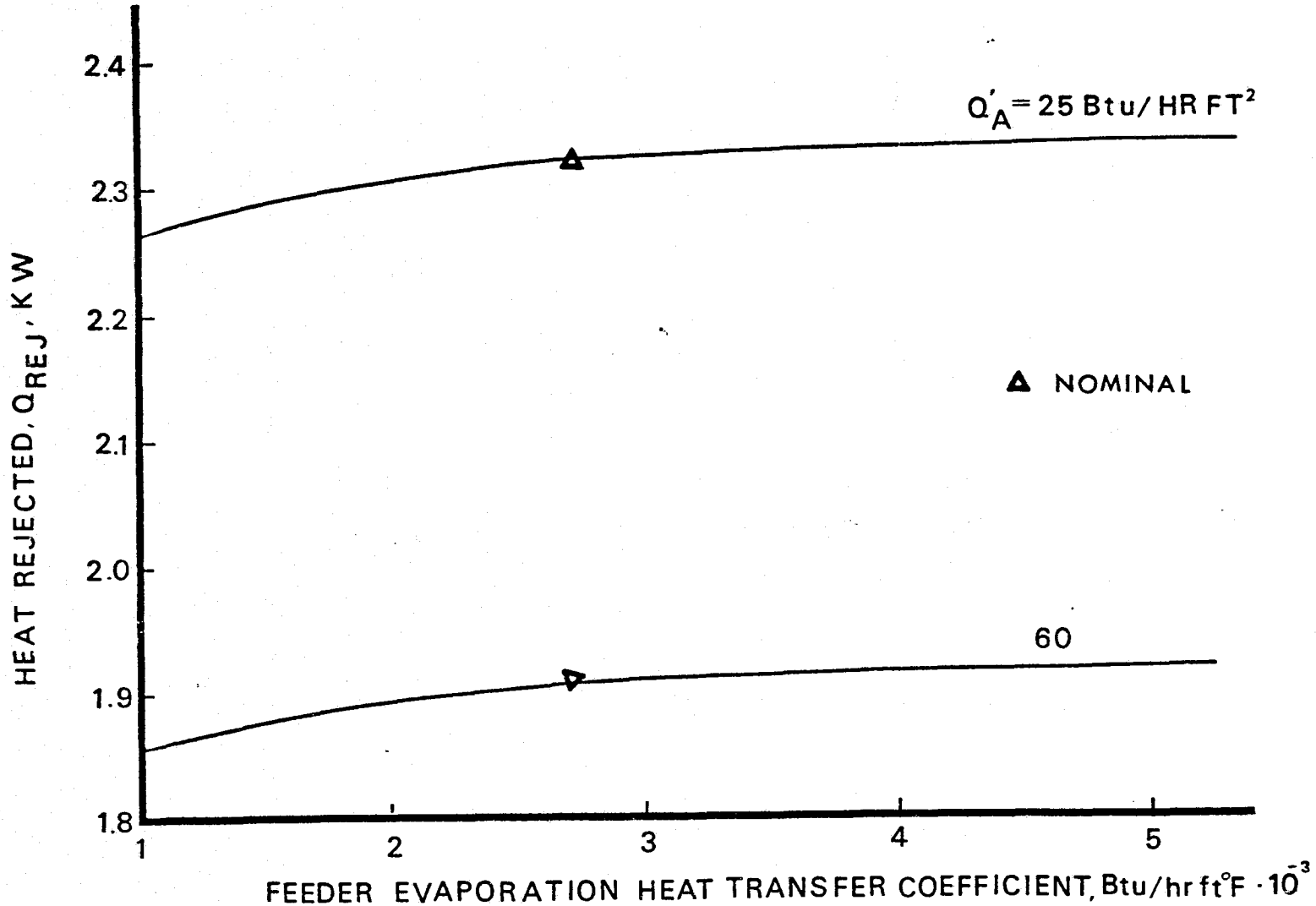

Figure 4.7 Q_{REJ} vs Heat Pipe Evaporation Heat Transfer Coefficient

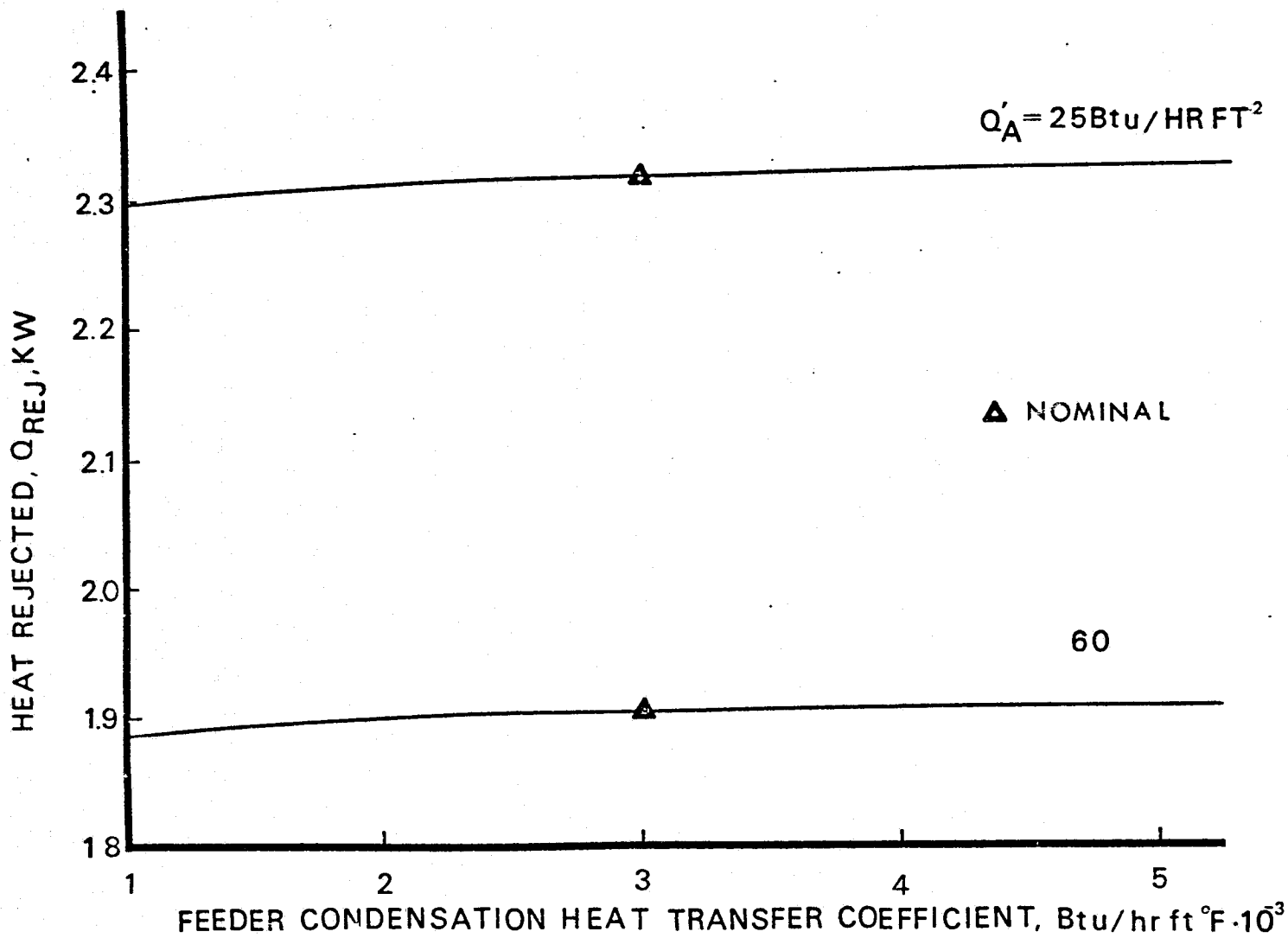

Figure 4.8 Q_{REJ} vs Heat Pipe Condensation Heat Transfer Coefficient

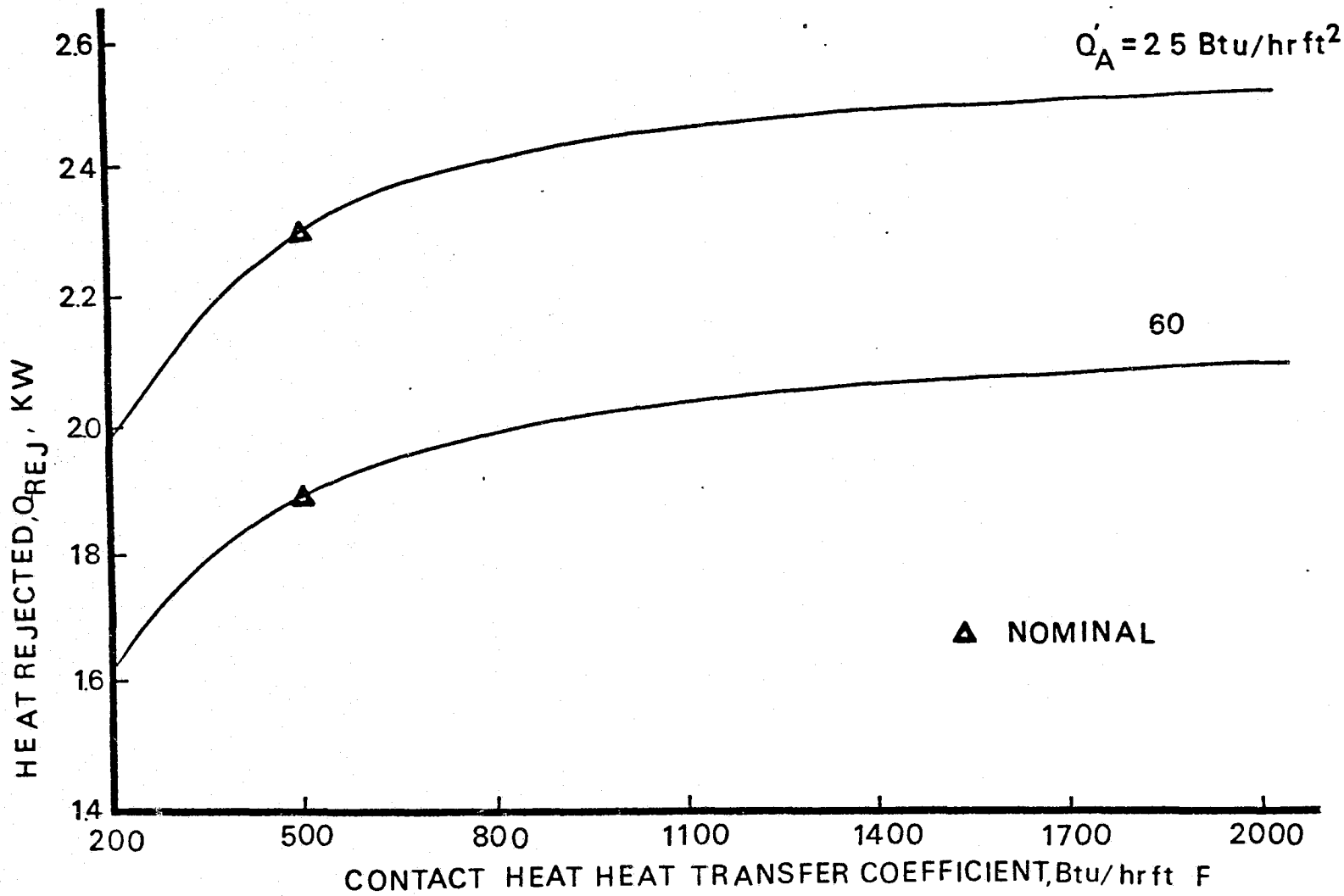

Figure 4.9 Q_{REJ} vs Contact Heat Transfer Coefficient between Heat Pipe and Panel

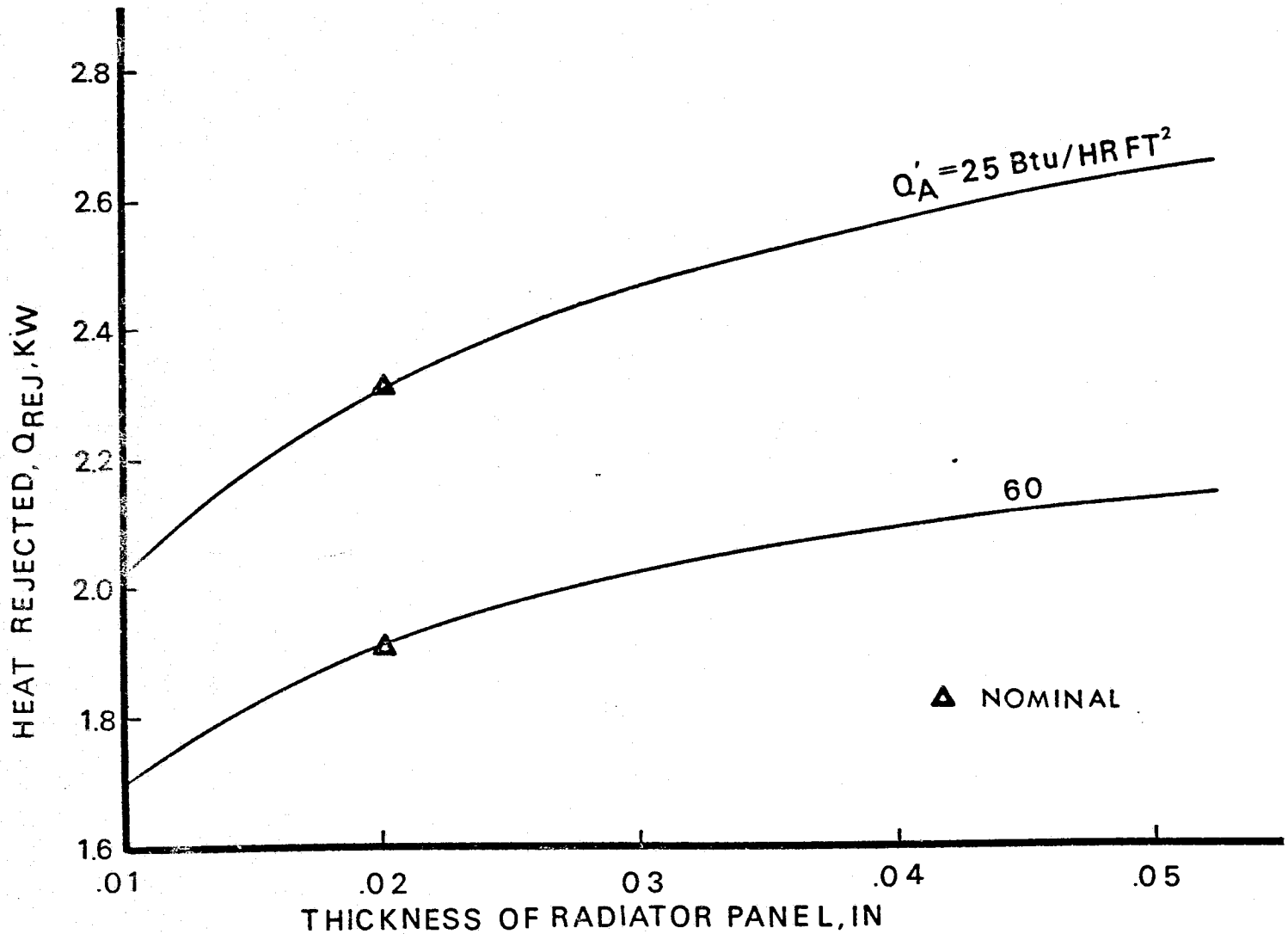

Figure 4.10 Q_{REJ} vs Panel Thickness

was assumed. The heat-pipe spacing was varied between 5.0 to 50.0 in with panel thicknesses of 0.01, 0.02 and 0.04 in. It was found, Figs. 4.11, 4.12 and 4.13, that the panel height ($=L_{chp}$) to width ($=N_pS$) ratio had negligible effect on the values of $(Q_{REJ}/W)_{opt}$ and S_{opt}. It is seen, however, that S_{opt} increases from 8 to 12.5 in., as the panel thickness increased from 0.010 in. to 0.040 in.

In the second case, the area of the panel was varied along with the heat pipe spacing, but a panel rejecting a constant amount of heat (1800 watts) was considered. Again, three panel thicknesses were assumed: 0.010, 0.020 and 0.040 in. Q/W versus the feeder heat pipe spacing, S, is shown in Fig. 4.14. From Fig. 4.14, it is seen that $(Q/W)_{opt}$ for each of the three panel thicknesses is the same as for the first case of a constant area panel.

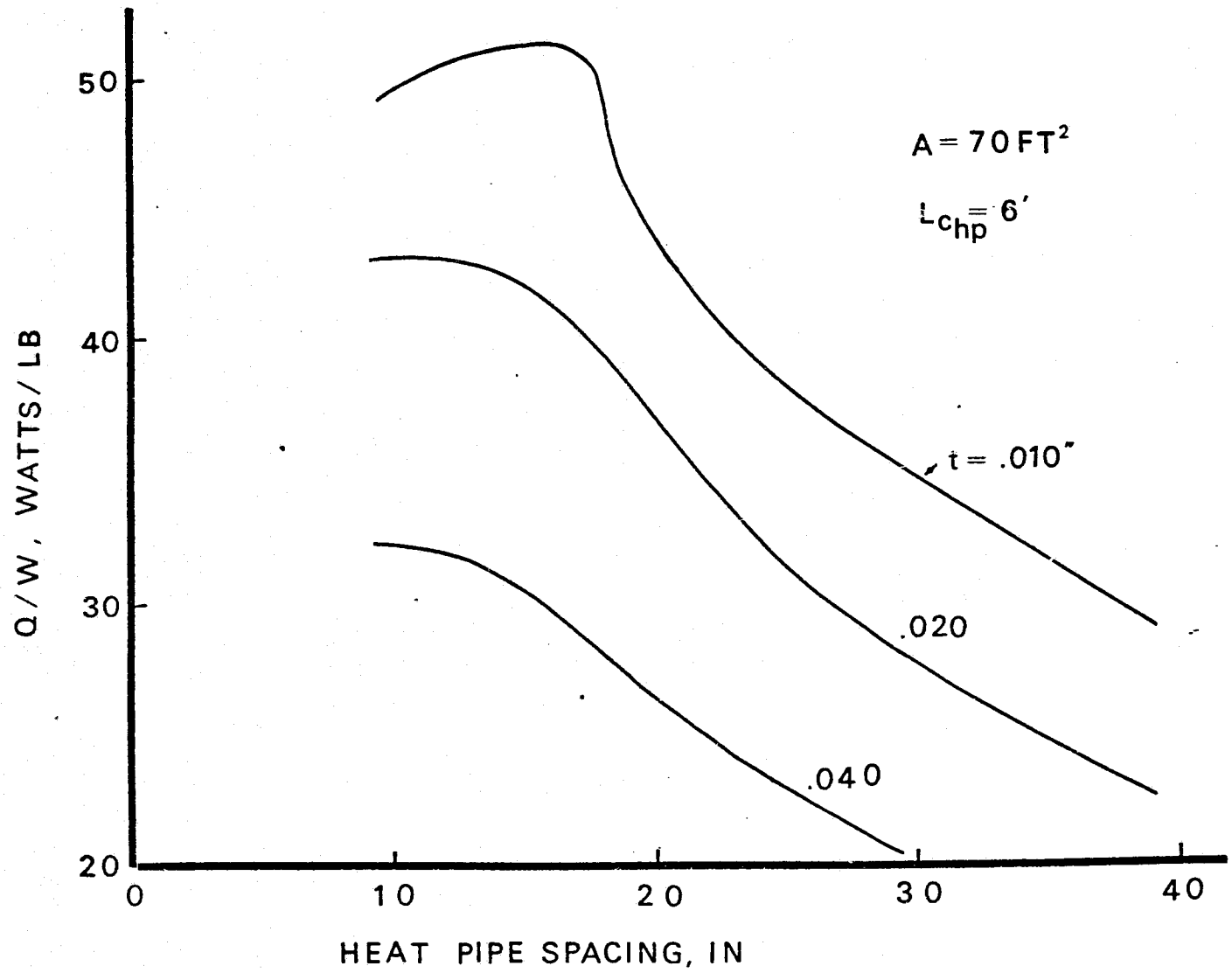

Figure 4.11 - Q_{REJ}/W vs Heat Pipe Spacing; A = 70 ft^2, $L_{c_{hp}}$ = 6'

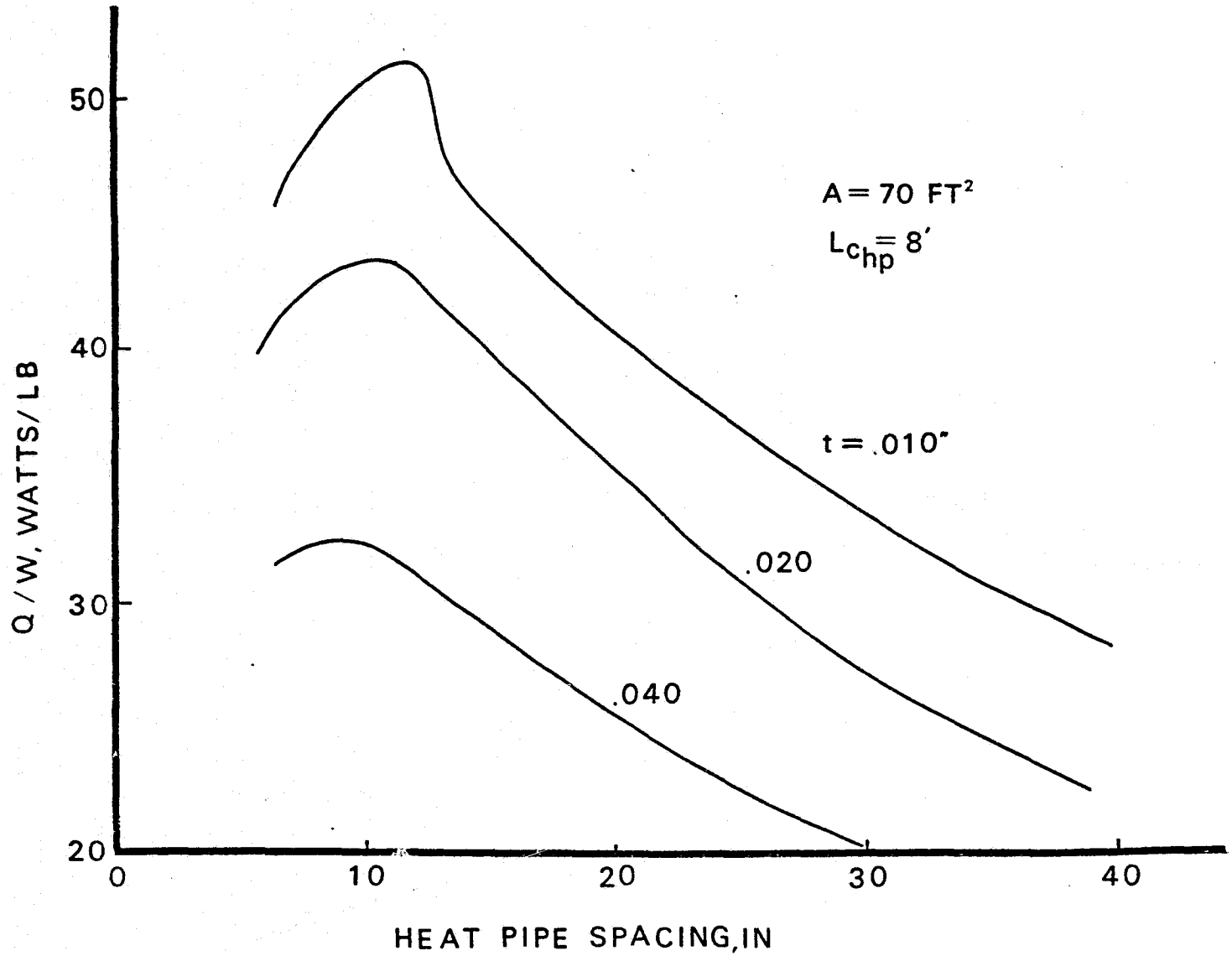

Figure 4.12 Q_{REJ}/W vs Heat Pipe Spacing; A = 70 ft^2, L_{chp} = 8'

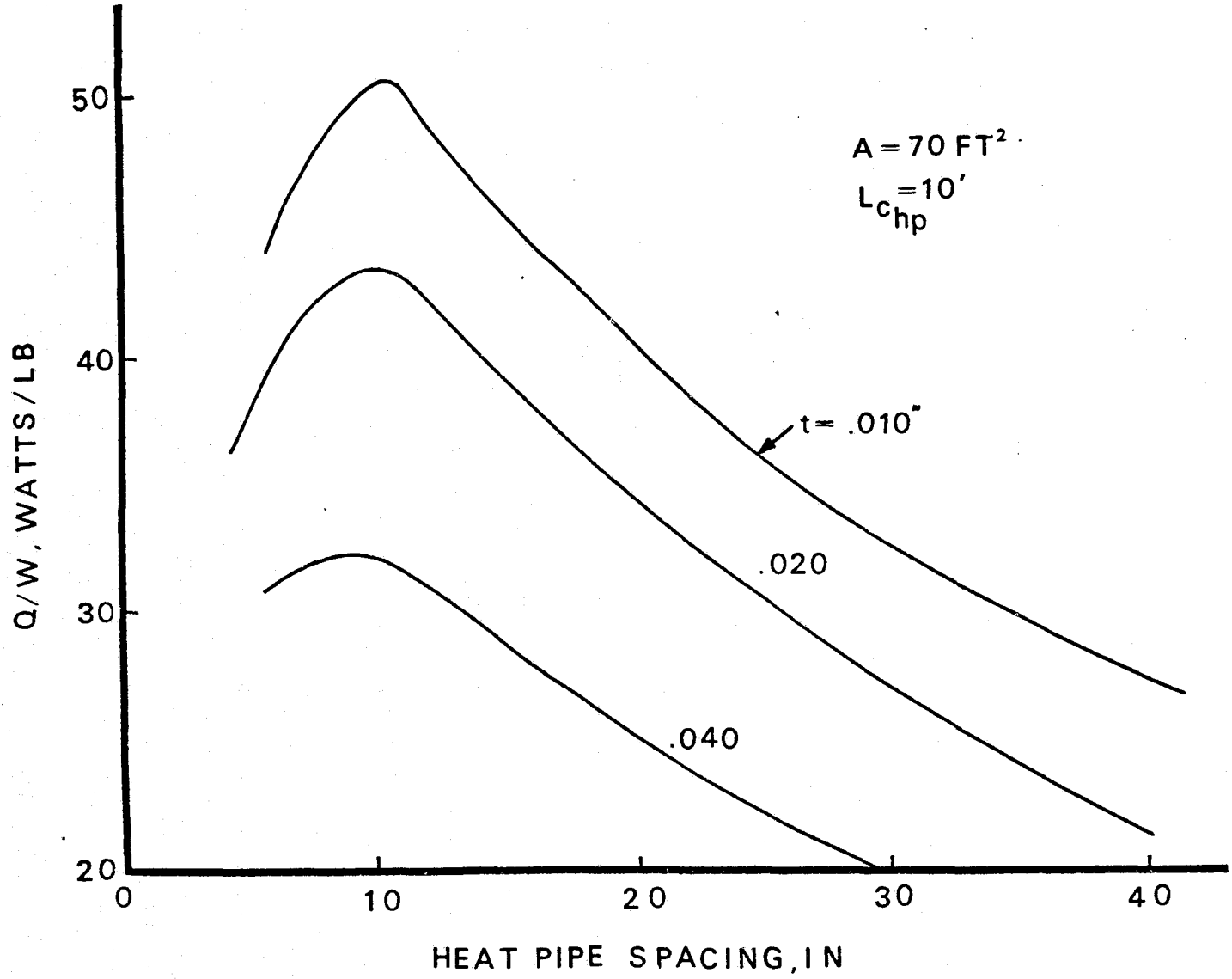

Figure 4.13 Q_{REJ}/W vs Heat Pipe Spacing; A = 70 ft^2, L_{chp} = 10'

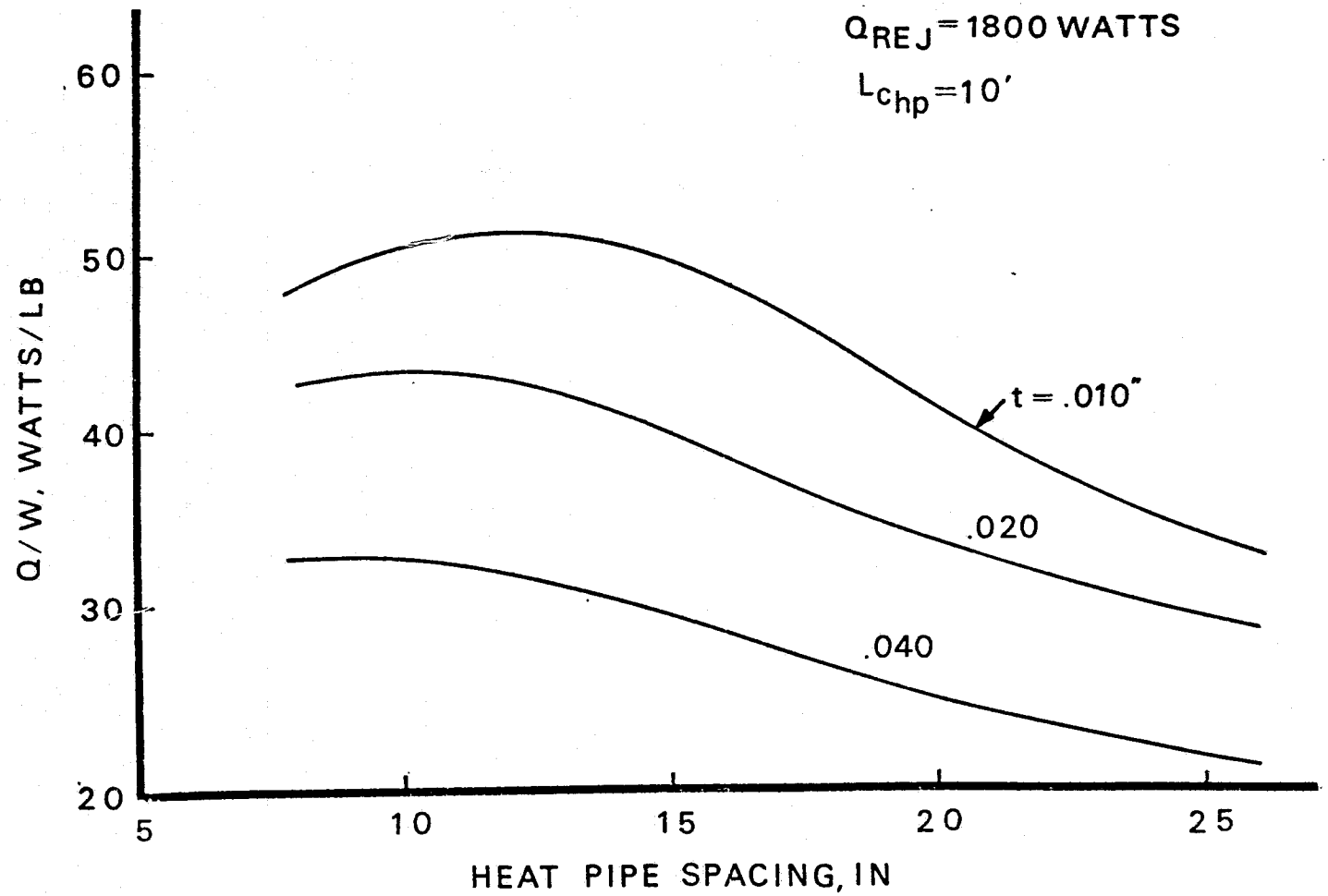

Figure 4.14 Q_{REJ}/W vs Heat Pipe Spacing; Q_{REJ} = 1800 W, L_{chp} = 10'

5.0 CONCLUSIONS

a. Rapid thawing of the VCHP header occurred when the temperature and flow of the Freon into the heat exchanger was increased to 40-50°F and 300-400 lb/hr, respectively ($Q'_A < 5.0 Btu/hr\,ft^2$). The feeder heat pipes did not thaw. After considerable delay, thawing of the feeders occurred; but thawing conditions were obscured by simultaneous changes of Freon and environmental conditions.

b. Similar to the thermal vacuum tests, the ambient study indicated the VCHP to be seriously heat-transport capacity limited.

c. An additional similarity between the vacuum and ambient tests was that the VCHP vapor temperature was greater than predicted, except at very low heat loads.

d. A ½ in. positive tilt of the VCHP condenser increased the active condenser length by 36% without an increase of the vapor temperature. The vapor temperature, however, was considerably greater than theoretical.

e. Supplemental heating of the VCHP also increased the active condenser length some, but at the same time the vapor temperature increased, which resulted in a larger departure from analytical predictions.

f. The finned fluid header radiator panel has an 8% higher theoretical capacity than a correctly functioning VCHP for the same operating conditions, surface area and feeder heat-pipe spacing.

g. The finned fluid header parametric and optimization studies revealed that the thinnest radiator fin (.010 in) yielded the highest Q/W values although a thicker fin increased the heat rejected.

h. For the prototype operating conditions, the optimum heat pipe spacing for maximum Q/W is approximately 11 in.

i. The most critical parameter from the standpoint of having greatest effect on the prototype performance was found to be contact width and heat transfer coefficient between feeder and panel.

j. When individual panels are connected in parallel, a dramatic improvement in heat rejection can be expected with finned fluid headers over VCHP headers.

6.0 RECOMMENDATIONS FOR FUTURE STUDY

Based on the results of the studies described in this report, the following recommendations for future study can be suggested:

1. Determine a means for lessening the thawing time of a heat pipe radiator panel such as the use of a selected number of low freezing point feeder heat pipes in selected panel locations.

2. A transient computer program for a fluid header heat pipe radiator is needed. The possibility of using a modified version of Lockheed's HPTRAN program (4) should be investigated. The final transient program should have provision for freezing and thawing of the feeder heat pipes.

3. The computations from a transient program when completed, as well as the steady state computer program described in Appendix C, should be compared with thermal vacuum test data when available.

4. The feasibility of building and using ultra-thin-wall panels (less than 0.020 in) should be considered for some applications, since they have high Q/W values.

7. APPENDICES

7.1 Test Data for Feasibility VCHP Header Ambient Supplemental Heating and Tilt Tests.

The parameter versus time plots for the data points of Table 3.1 are presented in Figure 7.1. Included are the parameters:

a. Reservoir temperature (2 sources)

b. Heat exchanger flow rate

c. Heat exchanger inlet temperature

d. Heat exchanger outlet temperature

e. Low conduction section temperatures:

LK03 ($\approx T_v$)

LK04

f. Heat exchanger delta temperature

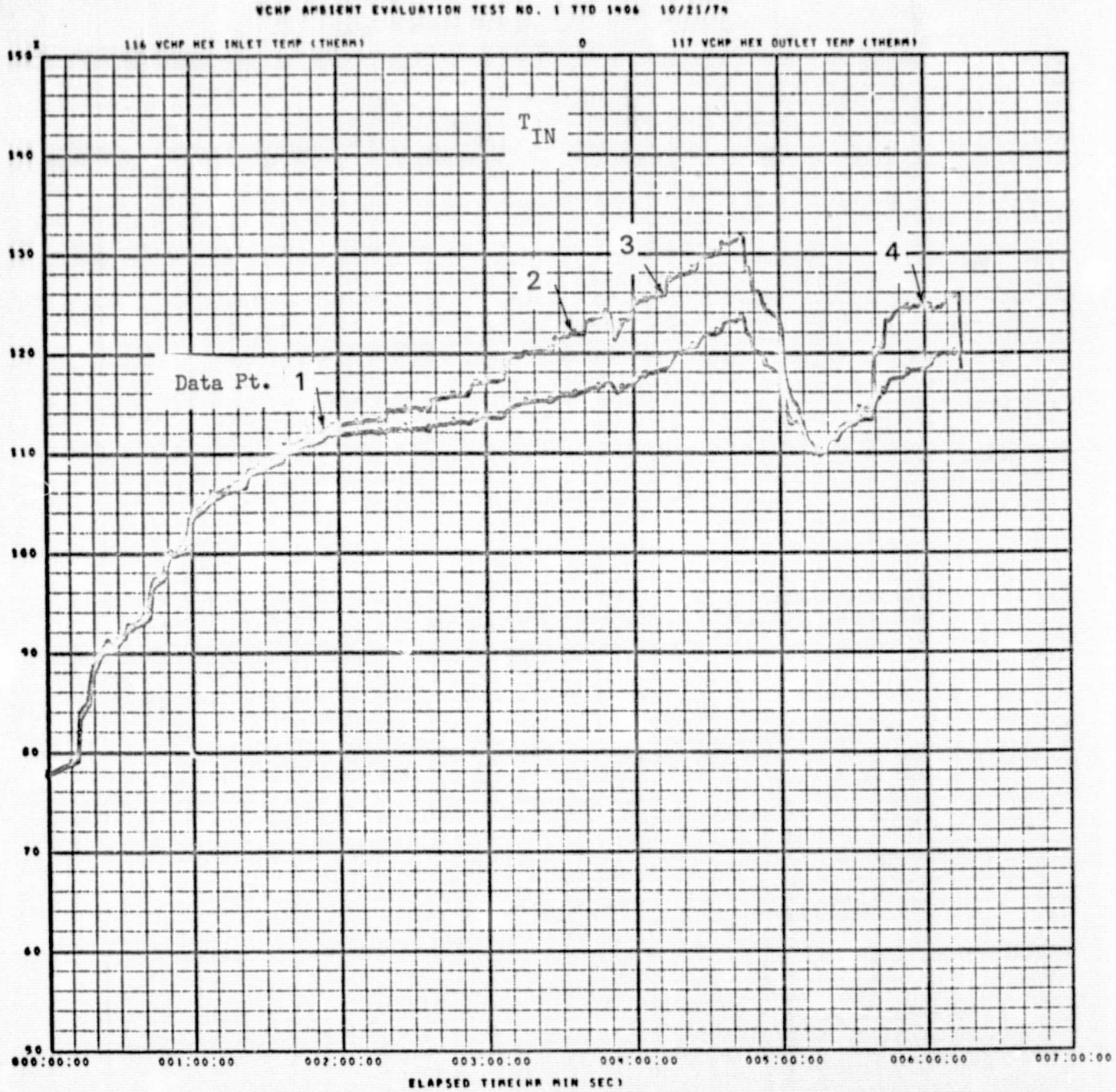

Figure 7.1 Parameter vs Time Plots for Feasibility VCHP Header Ambient Supplemental Heating and Tilt Tests

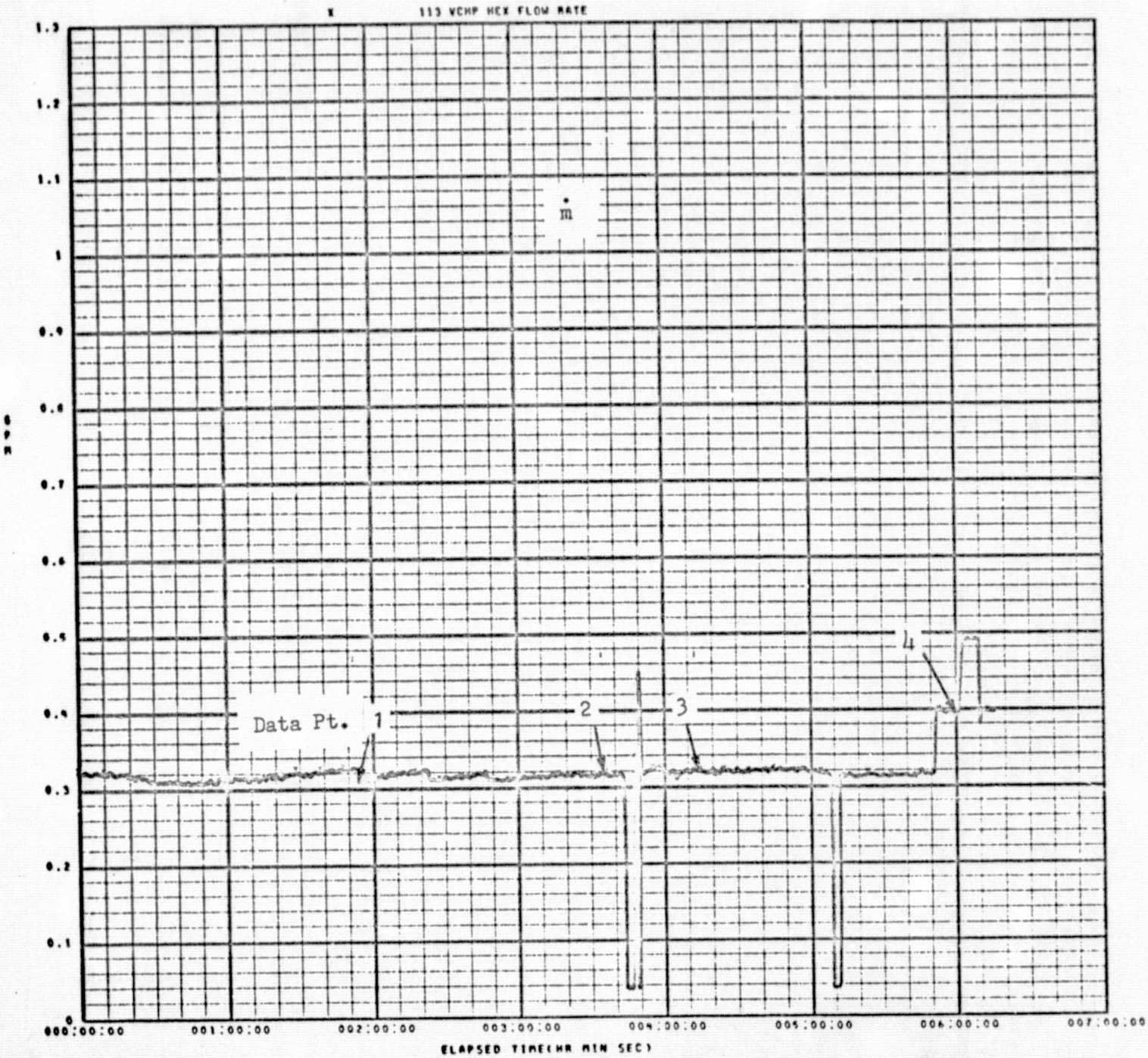

Figure 7.1 (cont.)

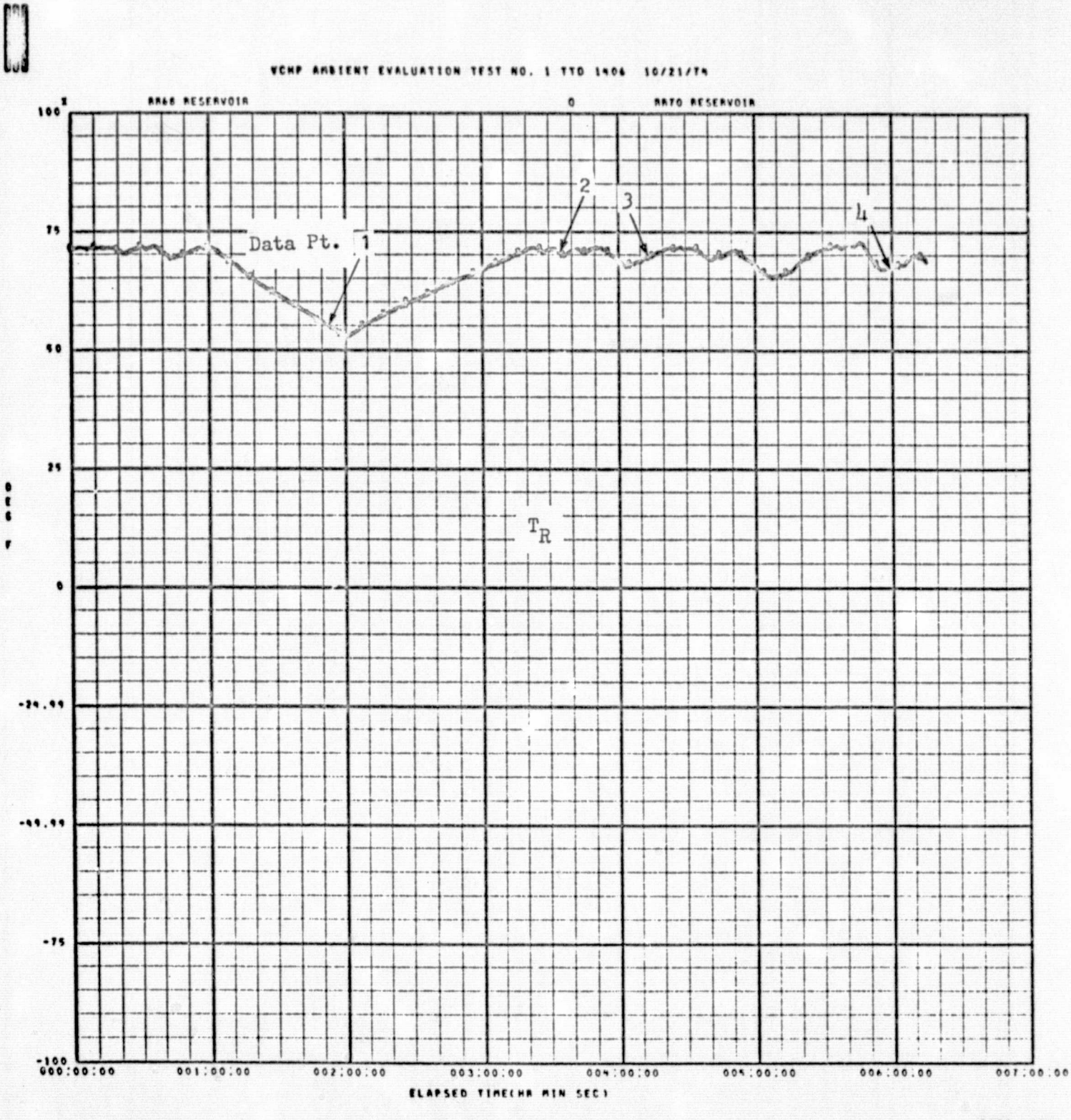

Figure 7.1 (cont.)

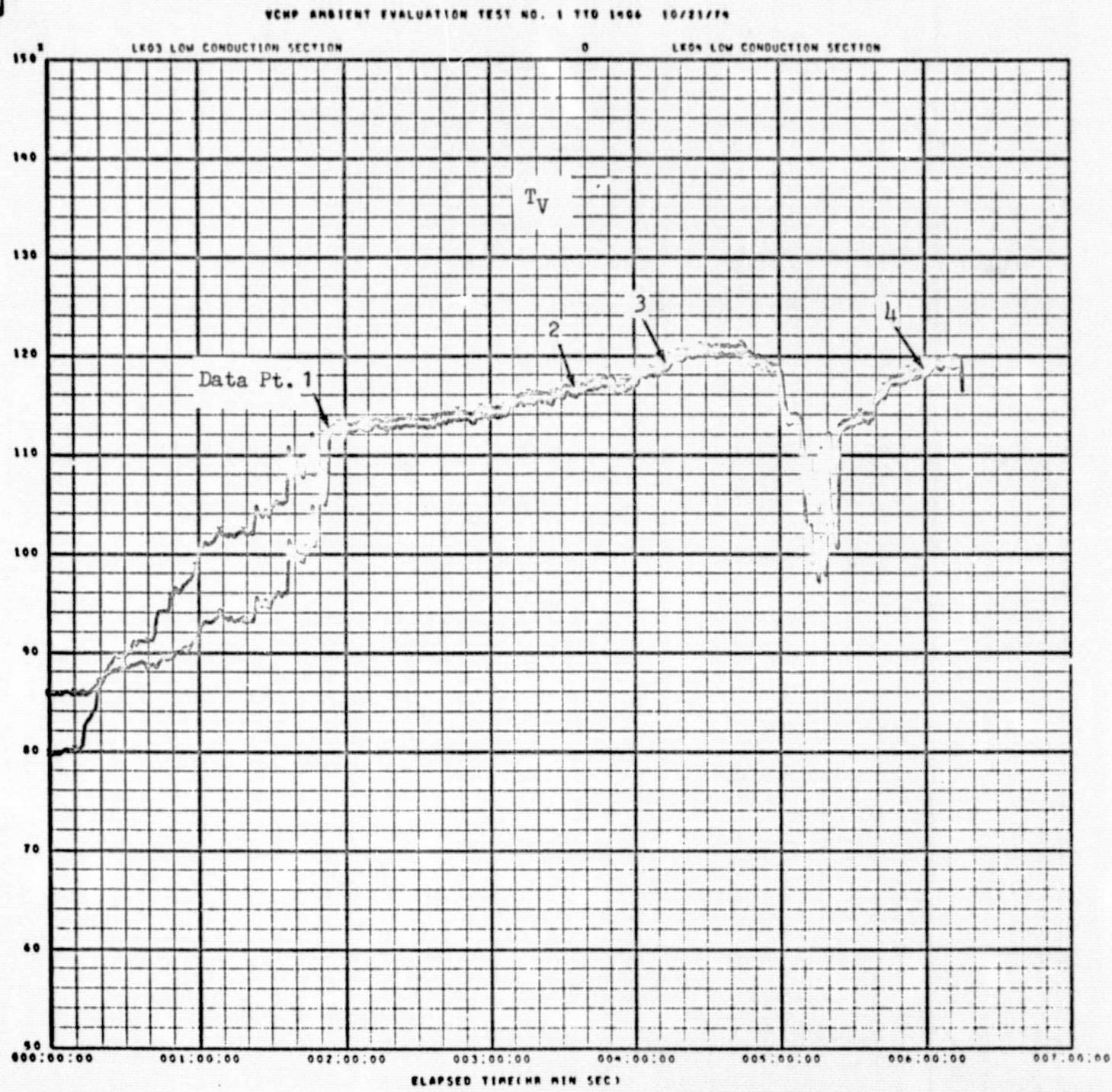

Figure 7.1 (cont.)

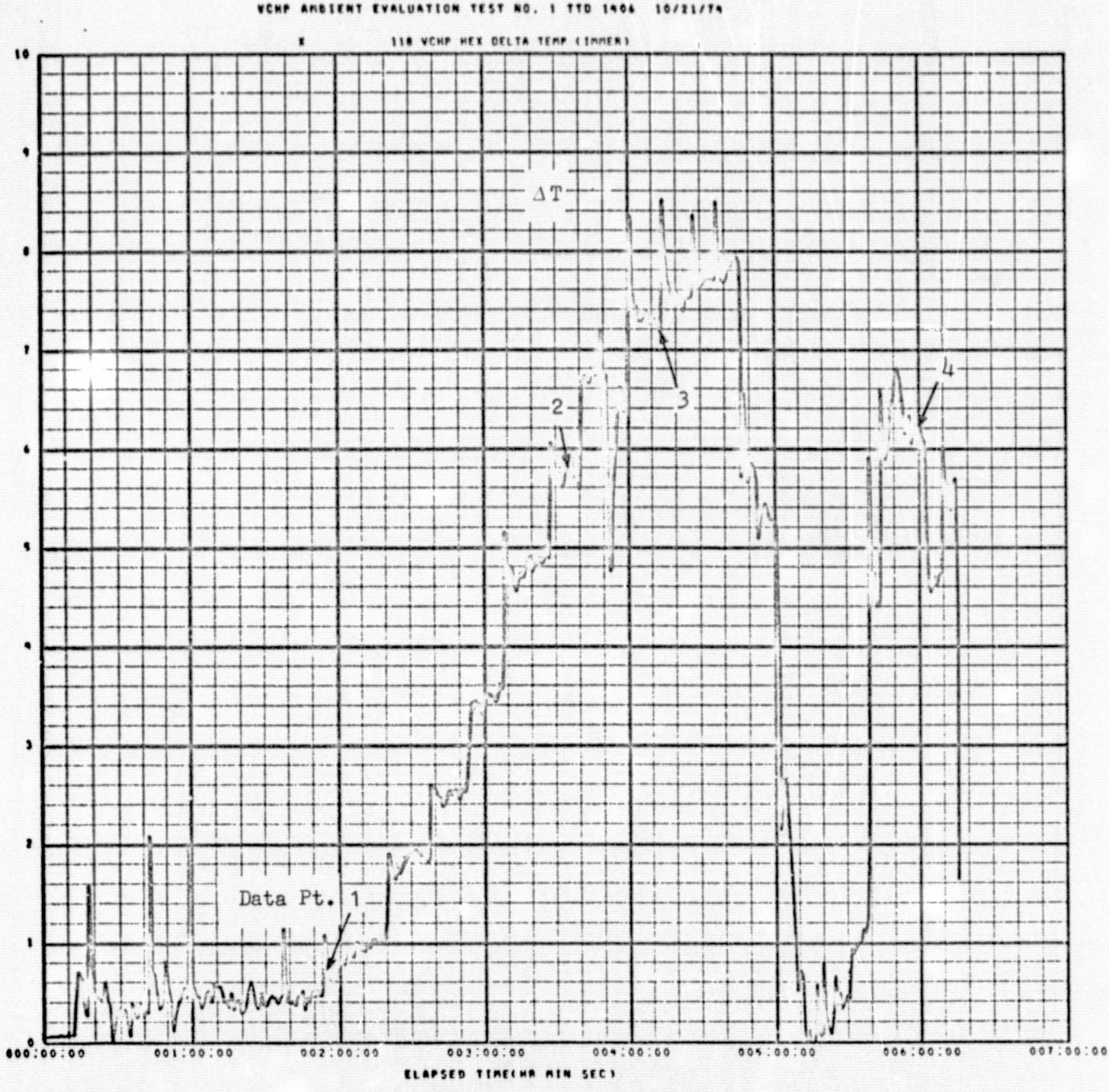

Figure 7.1 (cont.)

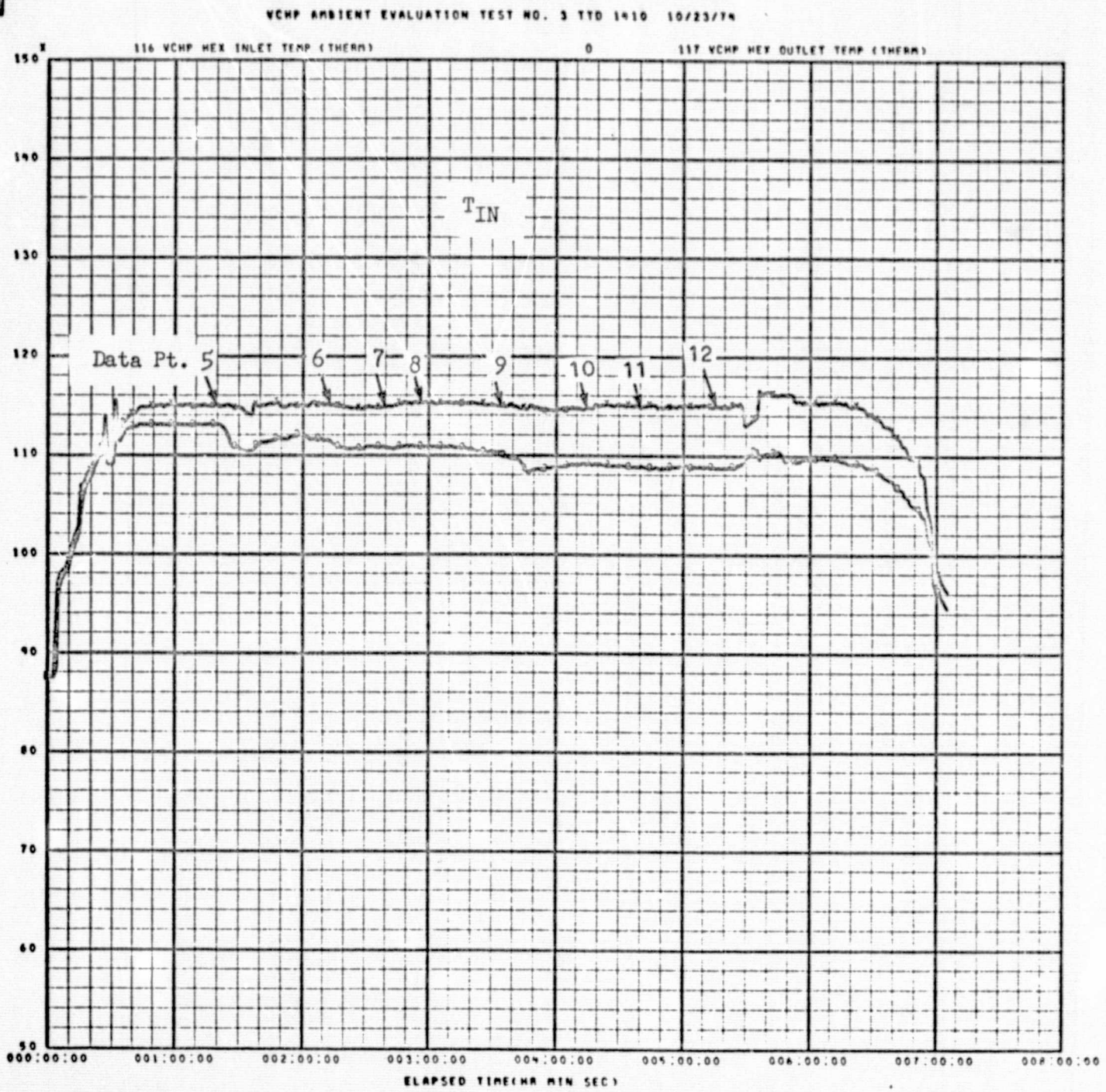

Figure 7.1 (cont.)

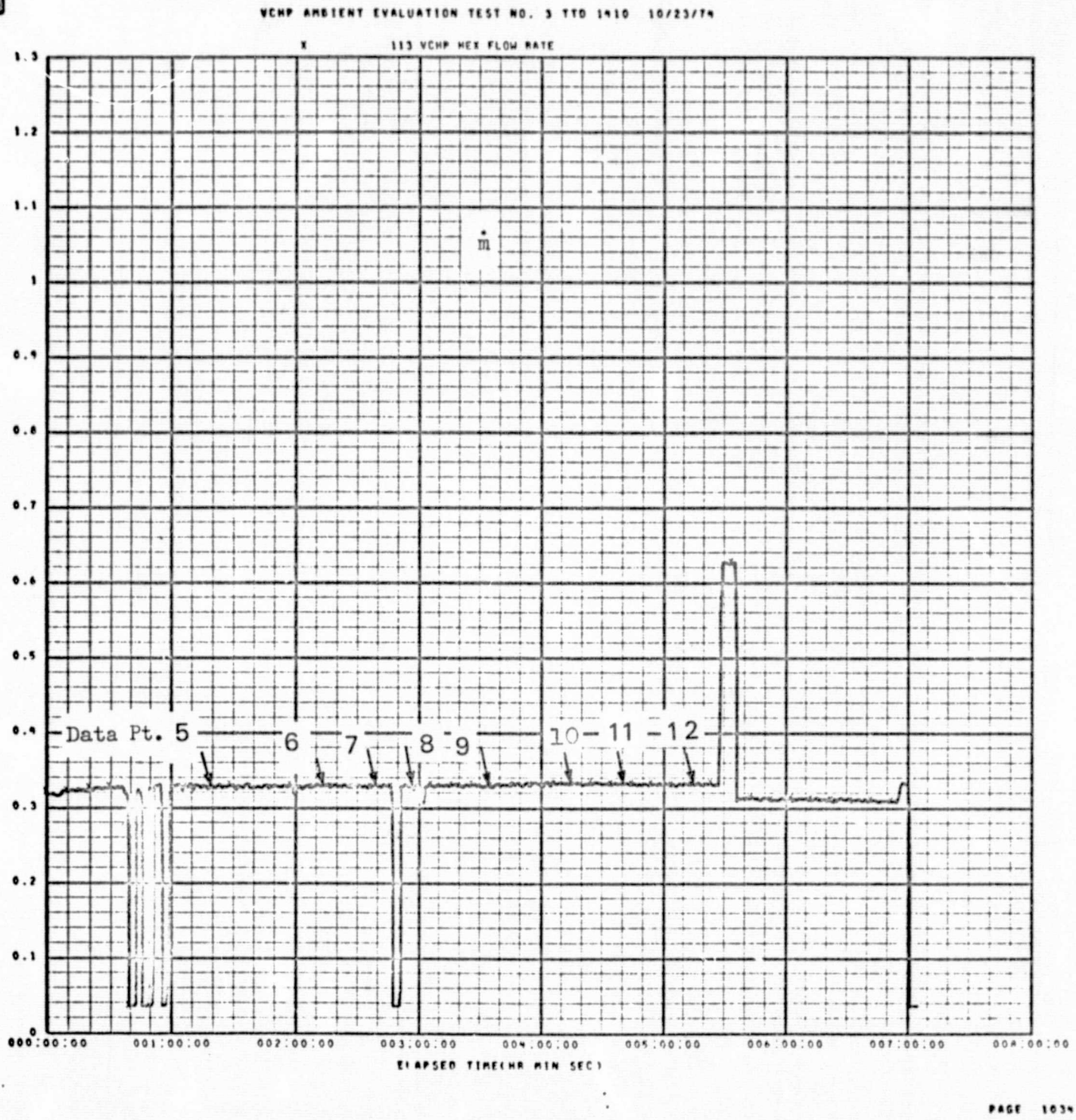

Figure 7.1 (cont.)

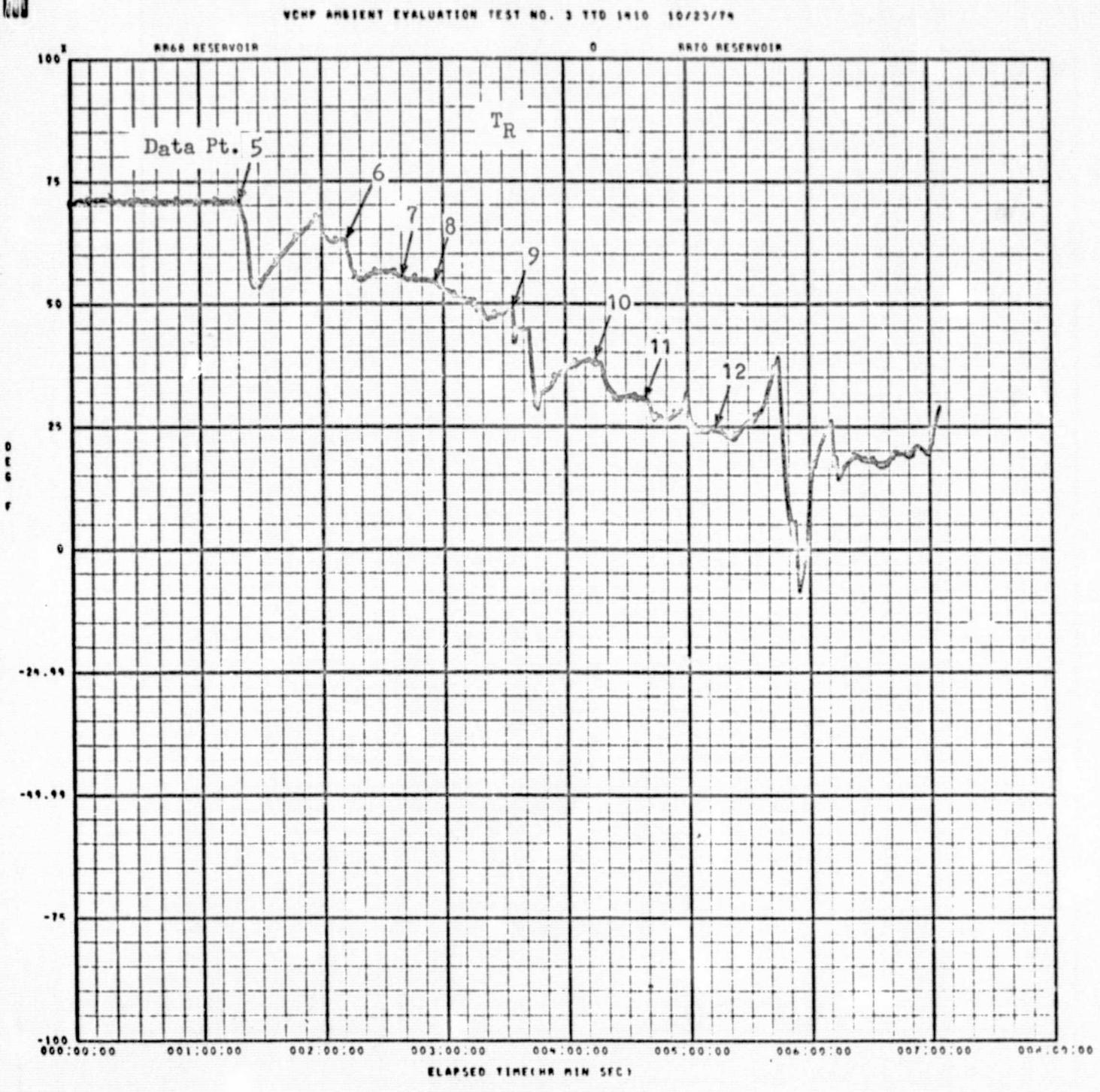

Figure 7.1 (cont.)

Figure 7.1 (cont.)

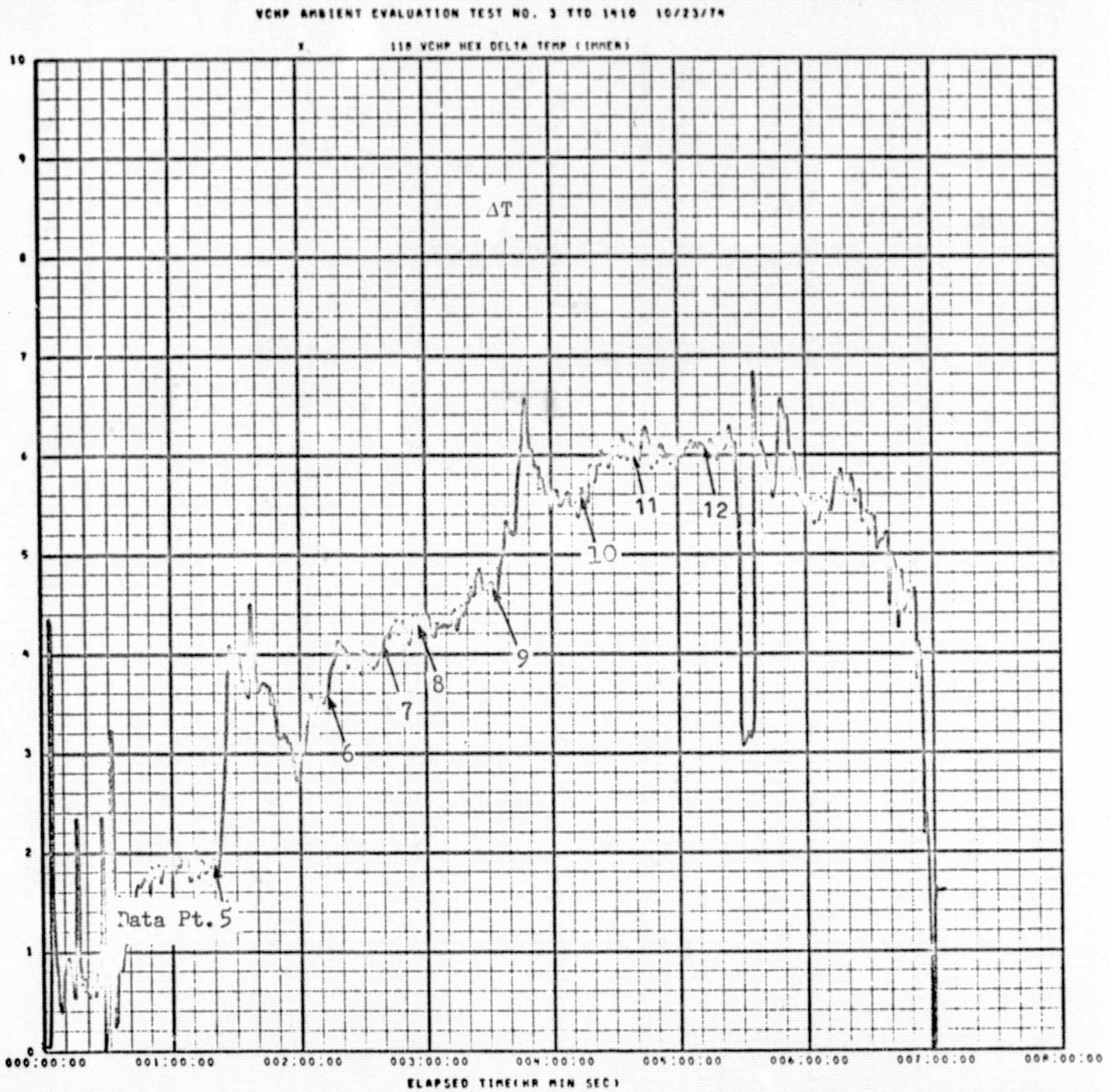

Figure 7.1 (cont.)

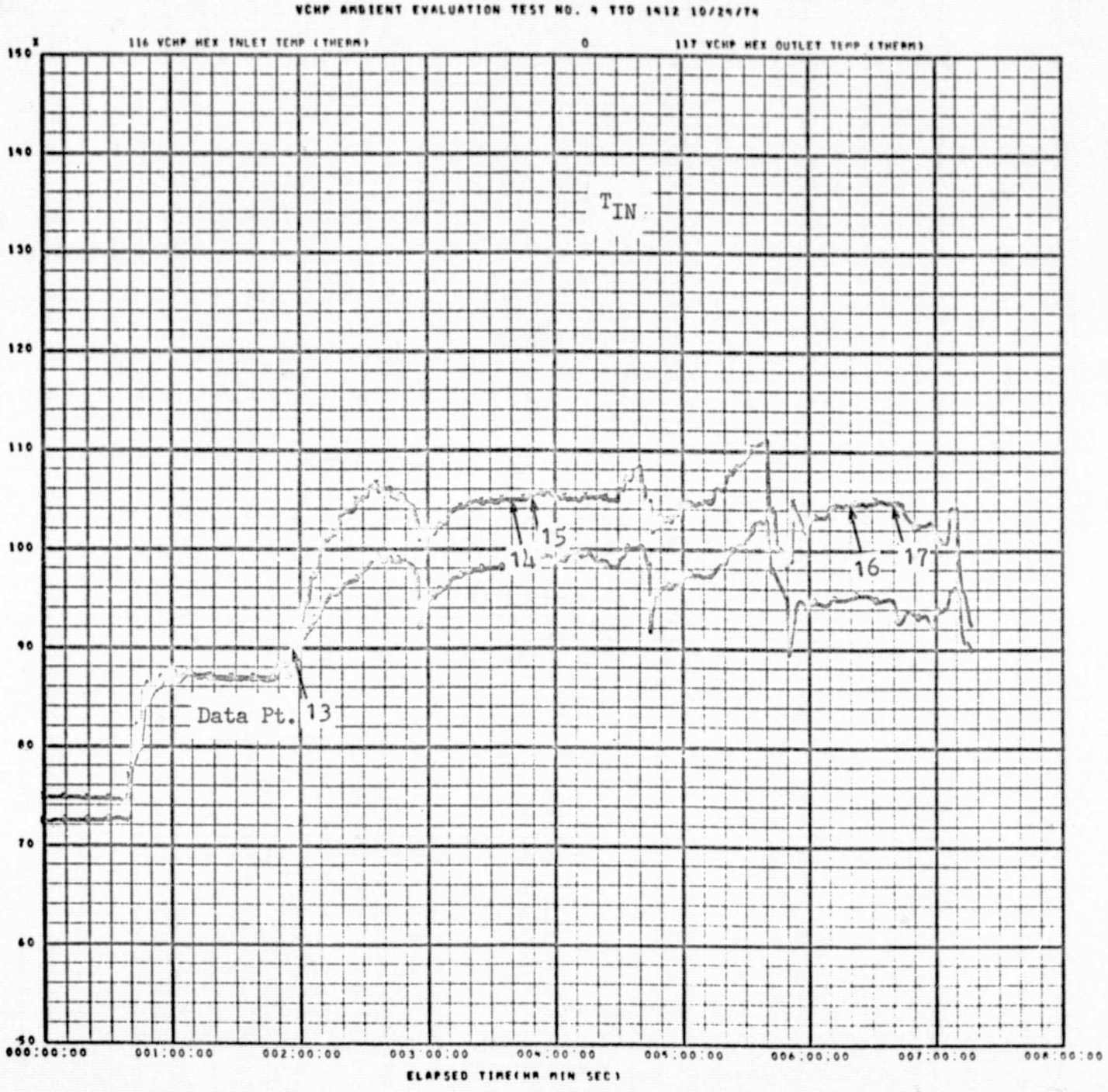

Figure 7.1 (cont.)

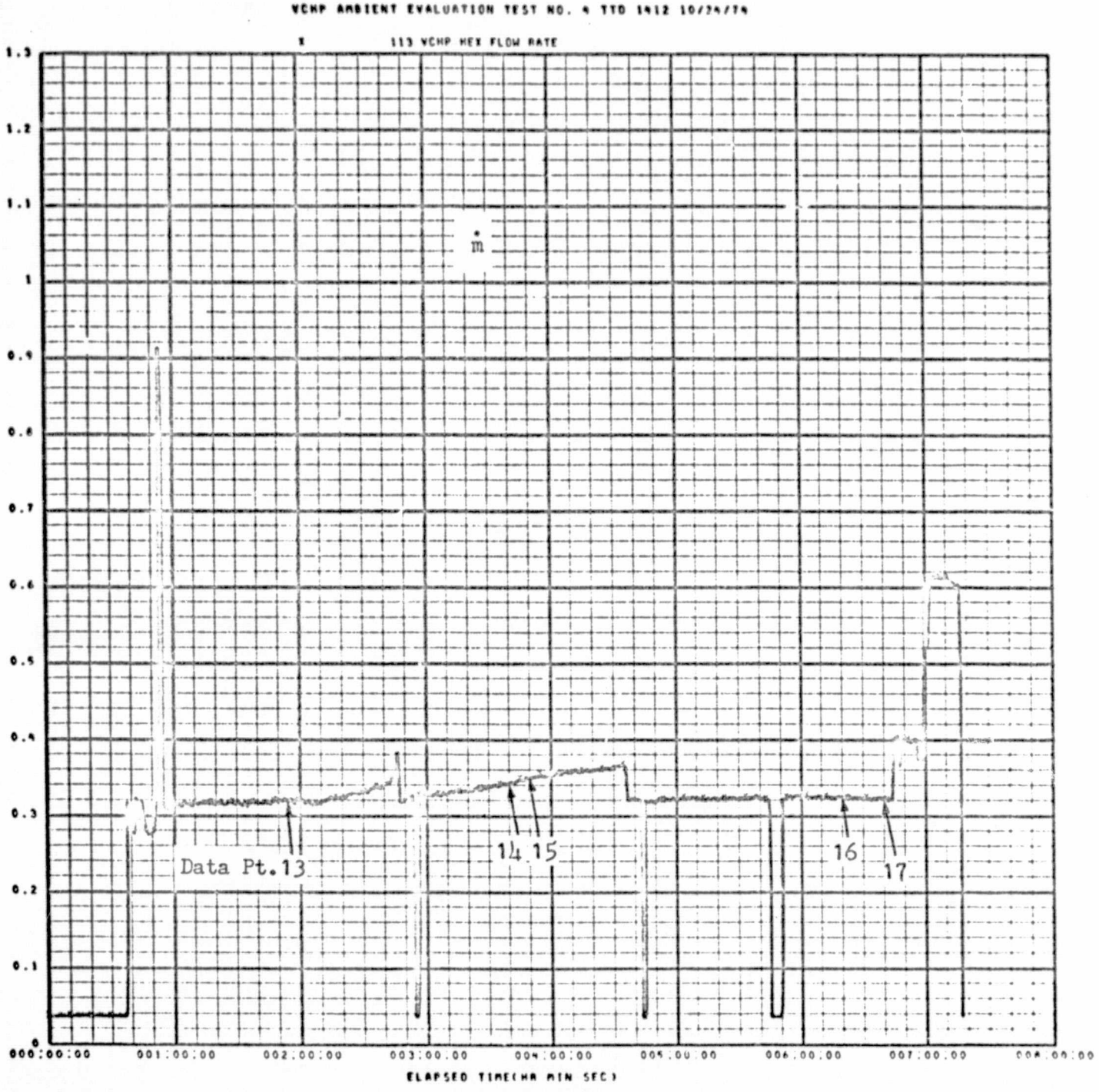

Figure 7.1 (cont.)

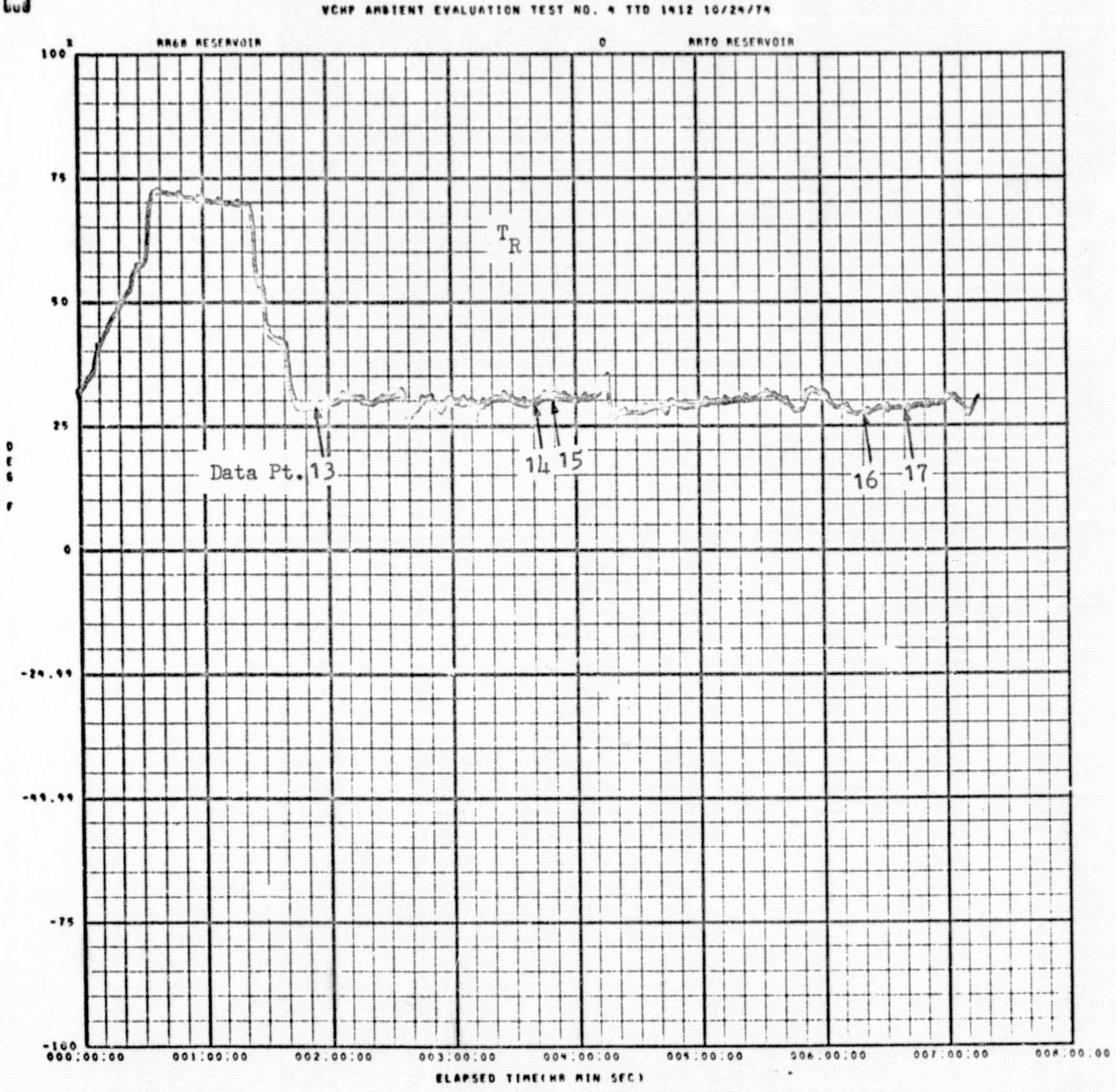

Figure 7.1 (cont.)

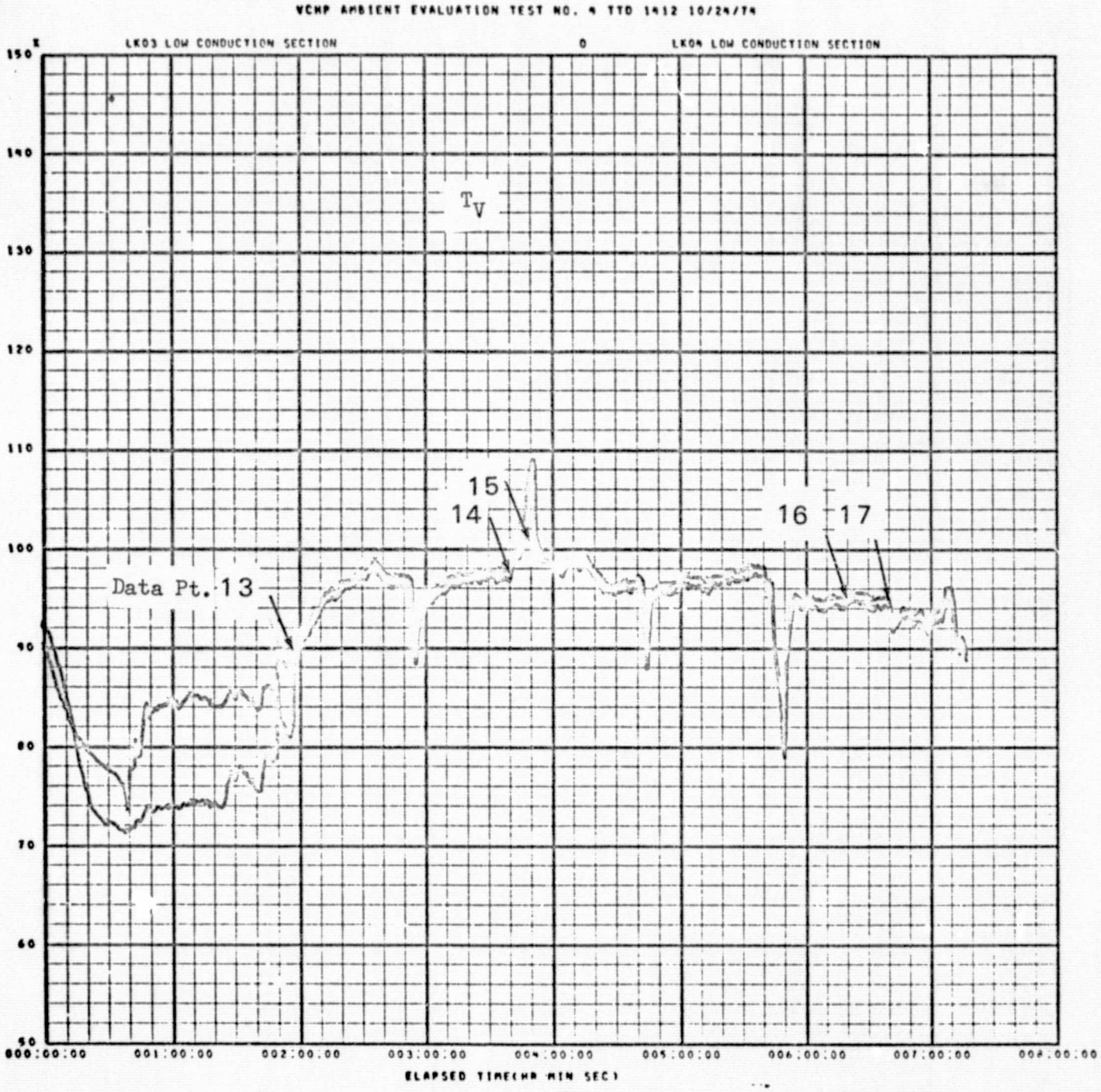

PAGE 1-07

Figure 7.1 (cont.)

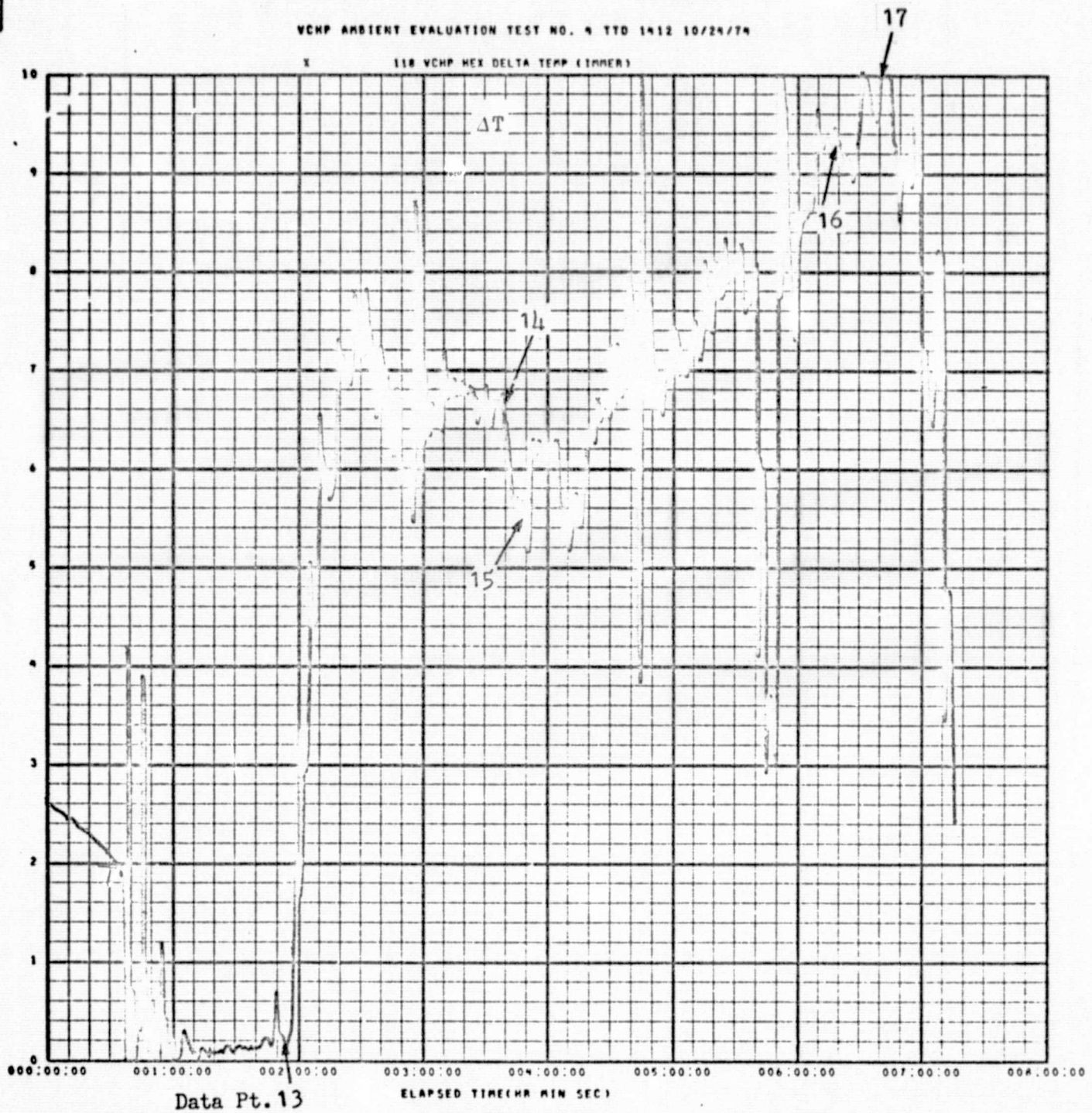

Figure 7.1 (cont.)

B. Conversion of Feasibility VCHP Into a Fluid Header

On the basis of the results from previous studies, the various heat transfer resistances depicted in Fig. 7.2 can be evaluated.

From reference 1, the resistances for the VCHP header feasibility panel are:

	Value (hr-°F/Btu)
$R_1 = 1/(h_o A_o \eta_o)$	.02442
$R_2 = 1/(he_{VCHP} \pi Di_{VCHP} L)$	.00768
$R_3 = 1/(h_3 \pi Di_{VCHP} \eta_3 Le_{hp})$	.01152
$R_4 = 1/(h_4 Le_{hp} w_4)$	.04
$R_5 = 1/(h_5 \pi Di_{hp} \eta_5 Le_{hp})$	.0071
$R_6 = 1/(h_6 \pi Di_{hp} Le_{hp} \eta_6$	.0005
$R_7 = 1/(h_7 Le_{hp} w_7)$	.012

From Sec. 4.0 of the present report, the heat transfer resistances for the fluid header panel are:

$$R_1 = 0$$

$$R_2 = 0$$

$$R_3 = 1/(h_o A_o \eta_o)$$

$$R_4 = 0$$

$$R_5 = 1/(h_5 \pi Di_{hp} Le_{hp})$$

$$R_6 = 1/(h_6 \pi Di_{hp} Le_{hp} \eta_6)$$

$$R_7 = 1/(h_7 Le_{hp} w_7)$$

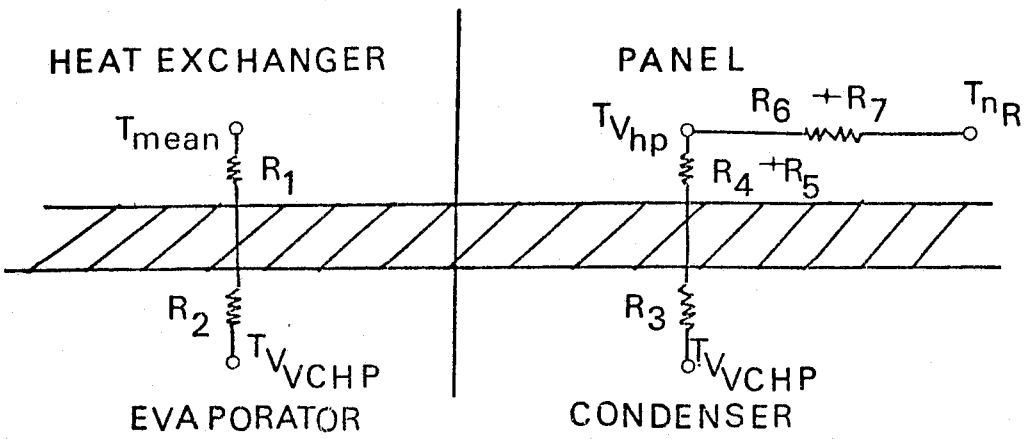

(b) VCHP FLUID HEADER

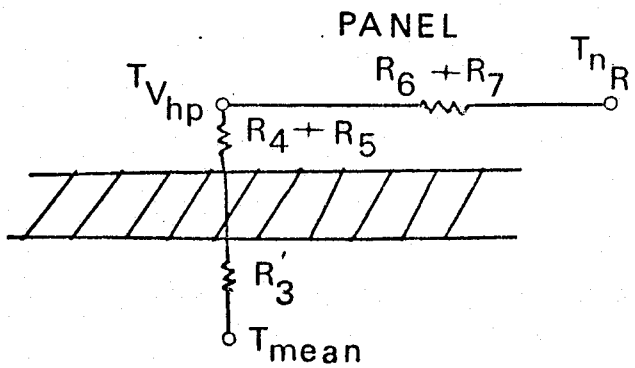

(a) FEASIBILITY FLUID HEADER

Figure 7.2 Heat Transfer Resistances

Combining the above to obtain the heat transfer resistances for the VCHP reworked to a fluid header:

$$R_1 = 0$$
$$R_2 = 0$$
$$R_3 = R_3' = 1/(h_o A_o \eta_o)$$
$$R_4 = 1/(h_4 L_{c_{lp}} w_4)$$
$$R_5 = 1/(h_5 \pi D_{i_{lp}} L_{c_{lp}})$$
$$R_6 = 1/(h_6 \pi D_{i_{lp}} L_{c_{lp}} \eta_6)$$
$$R_7 = 1/(h_7 L_{c_{lp}} w_7)$$

To compare the feasibility panel's analytical performance before and after its conversion from a VCHP to a fluid header, R_3' is set equal to the value of R_1 for the VCHP header, 0.02442 hr-°F/Btu. Then, the required coolant flow to produce a convective heat transfer coefficient equivalent to R_3' = 0.02442 hr-°F/Btu is determined. The heat transfer coefficient corresponding to the assumed value of R_3' is

$$R_3' = 1/(h_o A_o \eta_3) = 0.02442 \text{ hr-°F/Btu}$$

where

$$A = \pi D_{i_{VCHP}} L_{c_{VCHP}}$$

$$\eta_3 = .6 \text{ (assumed)}$$

Solving for h_o

$$h_o = 1/[\pi(\tfrac{.87}{12})(4)(.6)(.02442)]$$

$$= 449 \text{ Btu/hr ft}^2\text{°F}$$

The hydraulic diameter is defined:

$$D_h = \frac{4A}{WP} \qquad 7\text{-}1$$

Note that with the wick of the VCHP header remaining in place, the vapor volume of the VCHP header becomes the coolant internal volume. Thus,

$$V_c = A\, L_{a_{VCHP}} \qquad 7\text{-}2$$

Combining Eqs 7-1 and 7-2 gives

$$D_h = \frac{4V_c}{L_{a_{VCHP}}\, WP} = \frac{4V_R}{(V_R/V_c)\, WP\, L_{e_{VCHP}}} \qquad 7\text{-}3$$

where V_R and V_R/V_c are known values for the feasibility VCHP. The wetted perimeter is approximately

$$WP \cong 2\pi (D_{i_{VCHP}} - G) \qquad 7\text{-}4$$

where G is the height of the annular area formed by the wick and the header.

Combining Eqs 7-3 and 7-4,

$$D_h = 2V_R / \left[(V_R/V_c)\, \pi\, (D_{i_{VCHP}} - G)\, L_{a_{VCHP}}\right]$$

In the ambient tests the coolant was water with properties:

$k_\ell = .364$ Btu/hr ft °F

$\mu_\ell = 1.65$ lb$_m$/hr ft

$P_r = 4.52$

In addition,

$D_{i_{VCHP}} = .87/12$ ft

$V_R/V_c = 7.5$

$V_R = 40/1728$ ft^3

$L_{a_{VCHP}} = 4$ ft

$G \cong .09/12$ ft

The Nusselt number can be determined:

$$Nu = h_o D_h / k_\ell = h_o \, 2 V_R / [k_\ell (V_R/V_C) \pi (D_{i_{VCHP}} - G) L_{eVCHP}]$$

$$= \frac{449\,(2)\,(40/1728)}{364\,(7.5)\,\frac{\pi}{12}(.87-.09)4}$$

$$= 9.32$$

A Nusselt number of 9.32 is high for laminar flow and low for turbulent flow. Assuming a transitional Reynolds number of 2300,

$$R_c = \frac{(\frac{\dot{m}}{A}) D_h}{\mu_\ell} = \frac{\dot{m}\,4}{\mu_\ell WP} = 2300$$

Substituting Eq. 7-4 for the wetted perimeter and solving for $\dot{m}$,

$$\dot{m} = 2300\,\mu_\ell\, 2\pi (D_{i_{VCHP}} - G)/4$$

$$= 2300\,(1.65)\pi\,(.875-.09)/24$$

$$= 387.5\ lb_m/hr$$

$$= .64\ GPM$$

Thus, it can be concluded that with all other conditions similar, a water flow of 0.64 GPM would provide a fluid header heat transport capacity considerably higher than the VCHP header, due to the resistance R_3' being less than 0.2442 hr-°F/Btu and R_1 and R_2 both equal to zero.

A series of ambient tests made on the feasibility fluid header during July, 1975 established qualitatively the correctness of the above reasoning.

C. Fluid Header Heat Pipe Radiator Computer Program

The equations presented in Sec. 4.1 for describing a thermal model of a fluid header heat pipe radiator panel were programed in Basic language.

The program, Table 7-1, consists of a main program and a subroutine. The input data, Table 7-2, is read by the main program and all parameters initialized. An assumed initial temperature drop ($3^{o}F$) of the coolant is used for the first iteration. The Freon convective heat transfer is calculated using mean bulk properties. The thermal conductance of the panel = $(1/C1 + 1/C2)^{-1}$ is determined, and the heat pipe root temperatures computed. Radiating fin temperatures at each nodal point, and the feeder heat transport are obtained from the matrix inversion subroutine.

After each iteration, the new heat transport of each feeder is compared with the old value. When the agreement between old and new values for each feeder is less than .001, then the calculations are stopped and the results printed, Table 7-3.

Multiple panel results can be obtained by inputting in statement 161 (a) the number of parallel branches and (b) the number of panels in series in each parallel branch. For example,

161 DATA 1,1

is used for single panel calculations whereas

161 DATA 2,3

is an example for two parallel branches consisting of 3 panels in series in each branch with a total of 6 panels.

Table 7.1 Computer Program Listing

```
LIS
HPIQ

100  DIM A[23,23],B[23,23],Q[11,5],Y[1,23],T[11,4],X[23,1],Z[23,1]
102  DIM H[1,11],R[1,11],S[1,11],V[1,11],M[1,11]
110  READ D9,M1,C0,N9,H5
115  READ D1,L5,H6,L3,N6
120  READ H7,W7,D6,K4,C7
125  READ D7,K2,D,Z0,G
130  READ H1,E,C5,B0,D8
135  READ C8,F6,L7,Q8,T
136  MAT  READ U[21,3]
140  DATA 3,2000,.25,11,2700
145  DATA .0417,.75,3000,6.75,.6
146  DATA 500,.02083,.075,95,.87
147  DATA .0521,95,.0005,.00167,23
148  DATA 0,0,.9,491,.006633
149  DATA .9,.0088,10.074,60,150
150  DATA 130,480,149,128,458,148,125,435,147,122,415,145,119,385
151  DATA 142,117,373,141,113,351,140,110,338,139,108,323,138,105.5
152  DATA 312,137,102.5,300,135,99.5,289,131.5,96.5,277,130,93.5
153  DATA 268,128.5,91,257,126,88,249,123,85.5,240,121,82,230,119
154  DATA 79.5,221,116,77.5,214,113,74,203,110
160  READ Y,O
161  DATA 1,1
162  PRINT "SYSTEM WITH NUMBER OF BRANCHES=",Y
163  PRINT "PANELS PER BRANCH=",O
165  PRINT "TOTAL FLOW-LBS/HR",M1
170  M1=M1/Y
175  PRINT "FLOW PER BRANCH-LBS/HR",M1
180  PRINT "Q-ABS",Q8
200  FOR H7=200 TO 1400 STEP 300
210  PRINT
220  PRINT "H7=",H7
230  A3=B0*3.143*D8*((D6^2)-(D7^2))/16
240  A0=B0*3.143*L5*((D6^2)-(D7^2))/4
270  A5=C7*A0
330  B1=(D6-D7)/2
380  R2=1/(H5*3.143*D1*L5)
400  R6=2/(H6*3.143*D1*L3*N6)
410  R7=2/(H7*L3*W7)
```

```
420  C2=1/(R6+R7)
430  L9=(L7-(D7+2*Z0))/(G-1)
440  E1=((Q8*(10^8))/(C8*.1714))^.25
445  E2=E1-460
446  Z4=0
460  P9=-(K2*L3*Z0)/L9
466  PRINT
477  PRINT
480  FOR W=1 TO 0
481  IF W=1 THEN 485
482  T=T7
485  T0=T-D9
486  Q0=M1*C0*(T-T0)
487  PRINT "INLET TEMPERATURE FOR PANEL",W,"IS",T
490  P7=1
492  GOTO 498
495  P7=P7+1
498  Z2=0
499  G6=0
500  FOR I=1 TO N9
510  IF P7>1 THEN 570
520  Q[I,1]=Q0/N9
540  GOTO 580
570  Q[I,1]=Q[I,4]
580  IF I>1 THEN 620
600  T7=T
620  T8=T7-Q[I,1]/(M1*C0)
621  U1=(T8+T7)/20+1.5
622  U2=INT(U1)
623  U3=U[U2,2]*2.419/(10^3)
624  K1=U[U2,1]*5.782/(10^4)
626  R0=D8*M1/(U3*A3)
627  P0=C0*U3/K1
628  IF R0>2300 THEN 631
629  H[1,I]=1.86*K1*((R0*P0)^.333)*((2*D8/L5)^.333)/D8
630  GOTO 632
631  H[1,I]=.023*K1*(R0^.8)*(P0^.333)/D8
632  M2=(2*H[1,I]/(K4*D))^.5
633  M3=M2*B1
634  N5=(EXP(M3)-EXP(-M3))/((EXP(M3)+EXP(-M3))*M3)
635  N0=1-((1-N5)*(A5/A0))
636  R1=1/(H[1,I]*A0*N0)
637  C1=1/(R1+R2)
639  R[1,I]=R0
640  A8=C1*(T7-T8)/Q[I,1]
660  T[I,1]=(T7-T8*EXP(A8))/(1-EXP(A8))
```

```
680  T[I,2]=T[I,1]-Q[I,1]/C2
690  T7=T8
695  S[1,I]=T[I,1]
696  V[1,I]=T[I,2]

697  M[1,I]=C1
700  NEXT I
840  GOSUB 1200
900  FOR Z=1 TO N9
910  B5=Z*2
920  Q[Z,2]=Y[1,B5]
921  F4=.1714*(((T[Z,2]+460)/100)^4-(E1/100)^4)/(T[Z,2]-E2)
922  H3=C5*F4
923  A7=3.143*L3*(D7+2*Z0)/2
924  Q[Z,3]=H3*A7*(T[Z,2]-E2)
925  Q[Z,4]=Q[Z,2]+Q[Z,3]
930  Q[Z,5]=(Q[Z,1]-Q[Z,4])/Q[Z,1]
940  Z2=Z2+Q[Z,4]
950  NEXT Z
960  B6=1
970  IF ABS(Q[B6,5])>.001 THEN 495
980  B6=B6+1
990  IF B6>N9 THEN 1008
1000  GOTO 970
1008  Z3=Z2/3.4
1010  Z4=Z4+Z2
1011  P6=G6/N9
1017  PRINT "SOLUTION"
1018  MAT  PRINT Y;
1021  PRINT "OUTLET TEMPERATURE FOR THIS PANEL",T7
1025  PRINT "ROOT TEMPERATURES"
1026  MAT  PRINT V;
1027  PRINT "VAPOR TEMPERATURES"
1028  MAT  PRINT S;
1030  PRINT "HEAT REJECTED"
1031  PRINT Z2,"BU/HR"
1032  PRINT Z3,"WATTS"
1034  Z9=Z3/(L3*L7)
1035  PRINT "Q/A=",Z9,"WATTS/FT 2"
1040  NEXT W
1042  NEXT H7
1044  PRINT "THE TOTAL HEAT REJECTION FOR THIS BRANCH IS"
1045  PRINT Z4,"BTU/HR"
1050  Z5=Z4*Y
1055  PRINT "THE TOTAL HEAT REJECTION FOR THE SYSTEM IS"
1056  PRINT Z5,"BTU/HR"
```

```
1080  GOTO 3500
1200  FOR J=1 TO G
1210  IF B7=1 THEN 1360
1220  IF J=2 OR J=4 OR J=6 OR J=8 OR J=10 OR J=12 OR J=14 OR J=16 OR J=18 THEN 1770
1221  IF J=20 OR J=22 THEN 1770
1300  F2=.1714*(((Y[1,JJ+460)/100)^4-((E1/100)^4))/(Y[1,JJ-E2)
1310  H9=C5*F2
1320  O9=L3*L9*(H9+H1)
1330  Q9=O9-2*P9
1340  R9=L3*L9*(H9*E2-H1*E)
1350  GOTO 1770
1360  IF J>2 THEN 1390
1370  B7=1
1380  GOTO 1540
1390  IF J>4 THEN 1420
1400  B7=2
1410  GOTO 1540
1420  IF J>6 THEN 1450
1430  B7=3
1440  GOTO 1540
1450  IF J>8 THEN 1480
1460  B7=4
1470  GOTO 1540
1480  IF J>10 THEN 1501
1490  B7=5
1500  GOTO 1540
1501  IF J>12 THEN 1504
1502  B7=6
1503  GOTO 1540
1504  IF J>14 THEN 1507
1505  B7=7
1506  GOTO 1540
1507  IF J>16 THEN 1510
1508  B7=8
1509  GOTO 1540
1510  IF J>18 THEN 1513
1511  B7=9
1512  GOTO 1540
1513  IF J>20 THEN 1516
1514  B7=10
1515  GOTO 1540
1516  B7=11
1540  F2=.1714*(((T[B7,2]+460)/100)^4-((E1/100)^4))/(T[B7,2]-E2)
1550  H9=C5*F2
1560  O9=L3*L9*(H9+H1)
1570  Q9=O9-2*P9
```

```
1580  R9=L3*L9*(H9*E2-H1*E)
1770  FOR K=1 TO G
1780  IF K<J-1 OR K>J+1 THEN 1800
1790  GOTO 1820
1800  A[J,K]=0
1810  GOTO 2600
1820  IF J=2 OR J=4 OR J=6 OR J=8 OR J=10 OR J=12 OR J=14 OR J=16 OR J=18 THEN 1830
1821  IF J=20 OR J=22 THEN 1830
1825  GOTO 1940
1830  IF K=J-1 OR K=J+1 THEN 1860
1840  IF K=J THEN 1880
1860  A[J,K]=P9
1870  GOTO 1885
1880  A[J,K]=-1
1885  B3=J/2
1900  X[J,1]=(2*P9-09)*T[B3,2]+R9
1910  GOTO 2600
1940  IF J=1 THEN 1960
1950  GOTO 2030
1960  IF K=J THEN 2000
1980  A[J,K]=0
1990  GOTO 2005
2000  A[J,K]=Q9/2
2005  B3=(J+1)/2
2010  X[J,1]=R9-P9*T[B3,2]
2020  GOTO 2600
2030  IF J=G THEN 2050
2040  GOTO 2120
2050  IF K=J-1 THEN 2090
2070  A[J,K]=Q9/2
2080  GOTO 2095
2090  A[J,K]=0
2095  B3=(J-1)/2
2100  X[J,1]=R9-P9*T[B3,2]
2110  GOTO 2600
2120  IF J=3 OR J=5 OR J=7 OR J=9 OR J=11 OR J=13 OR J=15 OR J=17 OR J=19 THEN 2140
2121  IF J=21 THEN 2140
2130  GOTO 2600
2140  IF K=J-1 THEN 2170
2150  IF K=J THEN 2190
2160  IF K=J+1 THEN 2210
2170  A[J,K]=0
2180  GOTO 2220
2190  A[J,K]=Q9
```

```
2200  GOTO 2220
2210  A[J,K]=0
2220  B3=(J+1)/2
2221  B4=(J-1)/2
2230  X[J,1]=R9-P9*T[B3,2]-P9*T[B4,2]
2240  GOTO 2600
2600  NEXT K
2650  NEXT J
2700  MAT B=ZER[G,G]
2720  MAT B=INV(A)
2730  MAT Y=ZER[1,G]
2750  MAT Z=ZER[G,1]
2770  MAT Z=B*X
2790  MAT Y=TRN(Z)
3000  RETURN
3500  END
```

Table 7.2 Computer Program Input

PROGRAM SYMBOL	EQUATION SYMBOL	DESCRIPTION	VALUE
D9	T	$T_{out} - T_{IN}$ (For first iteration =	$3^{\circ}F$)
MI	$\dot{m}$	Freon flow rate	2000 lb/hr
CO	c_p	Freon specific heat	.25 Btu/lb $^{\circ}F$
N9	N_p	Number of heat pipes	11
H5	h_5	Evaporation heat transfer coefficient	2700 Btu/hr-ft^2-$^{\circ}F$
DI	D_{ihp}	Heat pipe inside diameter	.0417 ft
L5	L_{ehp}	Evaporator length	.75 ft
H6	h_6	Condensation heat transfer coefficient	3000 Btu/hr-ft^2-$^{\circ}F$
L3	L_{chp}	Condenser length	6.75 ft
N6	η_6	Condenser fin efficiency	.6
H7	h_7	Contact heat transfer coefficient	500 Btu/hr-ft^2-$^{\circ}F$
W7	w_7	Contact width	.0208 ft
D6	D_{ihx}	Fluid header inside diameter	.075 ft
K4	k	Fin thermal conductivity	95 Btu/hr-ft-$^{\circ}F$
C7	A_f/A_o	Fin Area to total surface area	.87
D7	D_{chp}	Heat pipe outside diameter	.0521 ft
K2	K_R	Panel fin thermal conductivity	95 Btu/hr-ft-$^{\circ}F$
D	δ	Evaporator fin thickness	.0005 ft
ZO	t	Panel fin thickness	.00167 ft
G	N	Number of nodal points	23
H1	h	Panel fin convective heat transfer coefficient	0 Btu/hr-ft^2-$^{\circ}F$
E	T_E	Convective environment temperature	0 $^{\circ}F$
C5	ϵ	Emissivity of panel fin	.9
BO	β	Heat transfer area per volume	491 ft^{-1}
D8	D_h	Hydraulic diameter	.006633 ft
C8	α	Absorptivity	.9

L7	L_p	Width of panel	10.074 ft
Q8	Q'_A	Absorbed heat flux	60 Btu/hr-ft^2
T	T_{IN}	Panel inlet temperature	150^{o}F

Table 7.3 Computer Program Output

```
RUN
HPIQ

SYSTEM WITH NUMBER OF BRANCHES=                1
PANELS PER BRANCH=             1
TOTAL FLOW-LBS/HR              2000
FLOW PER BRANCH-LBS/HR         2000
Q-ABS          60

H7=            200


INLET TEMPERATURE FOR PANEL    1            IS            150
SOLUTION
 63.6699     463.029     68.1696     454.749     67.8356     451.376
 67.3887     448.171     66.9414     444.957     66.4975     441.834
 66.0565     438.689     65.6161     435.583     65.1773     432.496
 64.735      429.744     64.1202     433.861     59.1428

OUTLET TEMPERATURE FOR THIS PANEL          139.005
ROOT TEMPERATURES
 107.581     107.229     106.516     105.804     105.091     104.391
 103.689     102.992     102.296     101.589     100.349

VAPOR TEMPERATURES
 145.357     144.389     143.396     142.411     141.432     140.471
 139.506     138.548     137.597     136.651     135.652

HEAT REJECTED
 5498.47       BU/HR
 1617.2        WATTS
Q/A=           23.7825       WATTS/FT 2

H7=            500


INLET TEMPERATURE FOR PANEL    1            IS            150
SOLUTION
 75.0553     548.271     79.4736     538.042     78.914      533.218
 78.2995     528.508     77.6919     523.917     77.0887     519.314
```

8.0 REFERENCES

1. Sellers, J.P., Jr., "Steady State Operation of a Heat-Pipe Radiator System: Analytical and Experimental", JSC-EC-R-74-1 L.B. Johnson Space Center, December 1973.

2. Sellers, J.P., Jr., "Steady State and Transient Operation of a Heat-Pipe Radiator System", HP-1, Tuskegee Institute, December 1974.

3. Swerdling, B. and Alario, J., "Heat Pipe Radiator: Final Report", HPR-14, Grumman Aerospace Corporation, October 1973.

4. Carroll, B.L., "User's Guide: Transient Variable Conductance Heat-Pipe Radiator System (HPTRAN)", TM 4016, Lockheed Electronic Company, Inc, Houston Aerospace Systems Division, February 1974.

9.0 SYMBOLS

A	Surface area, ft^2
A_c	Coolant free flow area, ft^2
A_f	Feeder evaporator fins total surface area, ft^2
A_o	Feeder evaporator total outside surface area, ft^2
b	Height of heat exchanger fins, ft
c_p	Specific heat of the coolant, Btu/lb-^oF
C1	Heat conductance = $1/(R_1 + R_2)$, Btu/hr-^oF
C2	Heat conductance = $1/(R_6 + R_7)$, Btu/hr-^oF
Di_{VCHP}	Inside diameter of VCHP header, ft
Di_{hp}	Inside diameter of feeder heat pipes, ft
D_{ohp}	Outside diameter of feeder heat pipes, ft
D_h	Hydraulic diameter, ft
Di_{hx}	Inside diameter of fluid header, ft
G	Coolant annulus gap, ft
h_3	VCHP header condensation heat transfer coefficient, Btu/hr-ft^2-^oF
h_4	Contact heat transfer coefficient between VCHP and feeder heat pipes, Btu/hr-ft^2-^oF
h_5	Feeder heat pipes evaporation heat-transfer coefficients, Btu/hr-ft^2-^oF
h_6	Feeder heat pipes condensation heat-transfer coefficients, Btu/hr-ft^2-^oF
h_7	Contact heat transfer coefficient between feeder heat pipe and panel, Btu/hr-ft^2-^oF
h_o	Convection heat-transfer coefficient for the coolant in the heat exchanger, Btu/hr-ft^2-^oF
h_{eVCHP}	Heat transfer coefficient for the evaporator portion of the VCHP header, Btu/hr-ft^2-^oF

h	Average convective heat transfer coefficient for the radiator panel, Btu/hr-ft^2-^{o}F
h_R	Radiation heat transfer coefficient for the radiator panel, Btu/hr-ft^2-^{o}F
k	Thermal conductivity of feeder evaporator fin material, Btu/hr-ft^2-^{o}F
k_l	Thermal conductivity of coolant, Btu/hr-ft-^{o}F
K_R	Thermal conductivity of radiator panel, Btu/hr-ft-^{o}F
L	Length of heat exchanger, ft
L_f	One-half of the feeder heat pipe pitch, ft
L_n	Distance between nodal points, ft
L_{chp}	Length of the condenser portion of feeder heat pipes, ft
$L_{c_{VCHP}}$	Length of the VCHP header, ft
L_{ehp}	Length of the evaporator portion of the feeder heat pipes, ft
$\dot{m}$	Flow rate of the coolant, lb/hr
m_g	Mass of the noncondensible VCHP gas, lb
N_p	Number of heat pipes on a panel
N	Number of nodal points
Nu	Nusselt number
Pr	Prandtl number
Q'_A	Absorbed heat flux, Btu/hr-ft^2
Q_n	Feeder half heat transport, Btu/hr
Q_{REJ}	Total heat rejected by the panel, Btu/hr
Q_{REJ_i}	Heat rejected by the ith feeder, equal to Q_i, Btu/hr
R_1	Feeder evaporator outside thermal resistance, hr-^{o}F/Btu

R_2 Thermal Resistance (See Fig 7-2), hr-^{o}F/Btu

R_3 Thermal Resistance (See Fig 7-2), hr-^{o}F/Btu

R_4 Thermal Resistance (See Fig 7-2), hr-^{o}F/Btu

R_5 Thermal Resistance (See Fig 7-2), hr-^{o}F/Btu

R_6 Condenser thermal resistance in feeder heat pipe, hr-^{o}F/Btu

R_7 Contact thermal resistance feeder heat pipe to panel, hr-^{o}F/Btu

Re Reynolds number

Rg Gas constant, lb_f-ft/lb_m-^{o}R

S Heat pipe spacing (=2 L_f), ft

t Thickness of radiator panels, ft

T_{adB} Adiabatic section temperature for feeder B of VCHP panel, ^{o}F

T_{BATH} Panel water coolant temperature (ambient tests only), ^{o}F

T_n Temperature of the panel at a nodal point, ^{o}F

T_{nR} Temperature of the panel at nodal point located on the feeder heat pipe envelope, ^{o}F

T_{IN} Temperature of the coolant as it enters the heat exchanger, ^{o}F

T_{OUT} Temperature of the coolant as it leaves the heat exchanger, ^{o}F

T_{mean} Mean temperature of coolant, ^{o}F

T_R Temperature of the VCHP reservoir, ^{o}F

T_s Temperature of vapor and gas in the inactive portion of the VCHP header condenser, ^{o}F

T_V Temperature of the vapor in the feeder heat pipe, ^{o}F

T_E Temperature of the convective environment, ^oF

T_E' Temperature of the Q_A' environment, ^oF

T_n Temperature of thepanel at the nth nodal point, ^oF

V_c VCHP header vapor and gas volume, ft^3

V_R Volume of the VCHP reservoir, ft^3

w_7 Contact width between heat pipe and panel, ft

WP Wetted perimeter, ft

β Transfer area per volume of theheat exchanger, 1/ft

σ Stephan-Boltzman constant = $.1714 \times 10^{-8}$ Btu/hr-ft^2-$^oR^4$

ΔT Coolant temperature drop, ^oF

δ Thickness of heat exchanger fins, ft

ϵ Emissivity of the radiator panel

η_6 Fin efficiency for heat transfer out of feeder condenser to radiator panel

η_3 VCHP header condenser fin efficiency

η_o Feeder evaporator total surface temperature effectiveness

μ_l Absolute viscosity of liquid, lb_m/ ft-sec

ψ Ratio of active length of VCHP header to total length